Hydrogeol J (2016) 24:35–57
DOI 10.1007/s10040-015-1323-5

REPORT

Investigation of recharge dynamics and flow paths in a fractured crystalline aquifer in semi-arid India using borehole logs: implications for managed aquifer recharge

M. Alazard[1,2] · A. Boisson[1,3] · J-C. Maréchal[2] · J. Perrin[3] · B. Dewandel[2] · T. Schwarz[1] · M. Pettenati[3] · G. Picot-Colbeaux[3] · W. Kloppman[4] · S. Ahmed[5]

Received: 3 October 2014 / Accepted: 2 October 2015 / Published online: 26 October 2015

Abstract The recharge flow paths in a typical weathered hard-rock aquifer in a semi-arid area of southern India were investigated in relation to structures associated with a managed aquifer recharge (MAR) scheme. Despite the large number of MAR structures, the mechanisms of recharge in their vicinity are still unclear. The study uses a percolation tank as a tool to identify the input signal of the recharge and uses multiple measurements (piezometric time series, electrical conductivity profiles in boreholes) compared against heat-pulse flowmeter measurements and geochemical data (major ions and stable isotopes) to examine recharge flow paths. The recharge process is a combination of diffuse piston flow and preferential flow paths. Direct vertical percolation appears to be very limited, in contradiction to the conceptual model generally admitted where vertical flow through saprolite is considered as the main recharge process. The horizontal component of the flow leads to a strong geochemical stratification of the water column. The complex recharge pattern, presented in a conceptual model, leads to varied impacts on groundwater quality and availability in both time and space, inducing strong implications for water management, water quality evolution, MAR monitoring and longer-term socio-economic costs.

Keywords Crystalline aquifer · Groundwater/surface-water relations · Groundwater flow · Conceptual model · India

✉ M. Alazard
marina.alazard@gmail.com

[1] Indo-French Centre for Groundwater Research, NGRI Campus, Groundwater Building, Uppal Road, 500007 Hyderabad, India

[2] BRGM, Water Environment and Ecotechnology Division, D3E Unit, Montpellier, France

[3] BRGM, Water Environment and Ecotechnology Division, D3E Unit, Orléans, France

[4] BRGM, Laboratory Division, Orléans, France

[5] National Geophysics Research Institute, Indo-French Centre for Groundwater Research, Hyderabad, India

Introduction

Despite their heterogeneity and limited yield, crystalline aquifers hold the primary water resource in many regions, especially in arid and semi-arid contexts where no surface water is available for much of the year. In India there are 26–28 million abstraction structures (Mukherji and Shah 2005; Shah 2009), and crystalline-aquifer groundwater represents more than 50 % of the groundwater used, mainly for agriculture, especially in South India (CGWB 2009; Saha et al. 2013). These aquifers suffer from over exploitation. Farmers are highly dependant on the small amount of water available (Aulong et al. 2012; Fishman et al. 2011), which is decreasing due to the rapid decreases of borehole yield and potential for storage with depth (Chilton and Foster 1995; Drew et al. 2001; Perrin et al. 2011a).

To counteract these problems and enhance water availability, in 1992, the Government of India launched, large and expensive programs of managed aquifer recharge (MAR) and rehabilitation of existing water conservation structures. To date, it is estimated that 0.5 million structures exist in the country with 0.25 million located on crystalline aquifers (Sakthivadivel 2007). The Central Ground Water Board recommends building 11 million recharge structures (CGWB 2007) and, for example, the former government of Andhra Pradesh (separated into Telangana and Andhra Pradesh since 2014) expects to increase aquifer recharge from 9 % in natural conditions to 15 % with MAR structures. Among the existing

structures, percolation tanks are largely represented. In India, 'percolation tank' is the name given to a small dam built on ephemeral rivers, where water is retained and infiltrates through the base to enhance recharge of the underlying unconfined aquifer. Generally, water for irrigation purposes or for village water supply is subsequently extracted from this aquifer.

However, numerous authors (e.g. Calder et al. 2008; Dillon 2009; Glendenning et al. 2012; Kumar et al. 2006; Oblinger et al. 2010) point out the lack of data at the local scale to allow a clear assessment of the structures' efficiency. This lack of knowledge on the efficiency impact of the MAR structures is recognized to be a major limitation of the MAR projects (Batchelor et al. 2003; Kerr et al. 2002; Kumar et al. 2008) and creates downstream externalities as the net benefits of the re-allocation from a downstream surface water irrigation system to a MAR structure upstream can be insufficient (Bouma et al. 2011). A growing body of studies quantifies the efficiency of these structures (e.g. Gale et al. 2006; Massuel et al. 2014; Metha and Jain 1997); however, only a few take into account groundwater evolution (i.e. de Silva and Rushton 2007; Gore et al. 1998; Massuel et al. 2014; Oblinger et al. 2010).

Given the heterogeneity of the crystalline-aquifer system—with important anisotropy (Maréchal et al. 2004; Sukhija et al. 2006), water-level-dependent connectivity (Guihéneuf et al. 2014) and lack of certainty about vertical flow (Boisson et al. 2015)—recharge processes are known to be a complex conjunction of diffuse piston flow and preferential flow paths (Athavale et al. 1983; Rangarajan and Athavale 2000) with both vertical and horizontal components. The need for a better understanding of the groundwater and recharge flow paths in crystalline aquifers is of scientific and social importance.

In addition to the efficiency issue, one major area where there is lack of knowledge relates to the impact of MAR structures on water quality. Despite a few studies published over the last years (e.g. Adhikari et al. 2013), chemical data are very scarce but are needed for developing and validating geochemical models, as in the case of fluoride studied by Pettenati et al. (2014). Identification and understanding of recharge flow paths is required at the structure scale. Numerous studies have shown the heterogeneity of recharge flow paths in heterogeneous media (e.g. de Vries and Simmers 2002; Herczeg and Leaney 2011; Scanlon et al. 1997, 2006; Simmers 1997), but mostly these are studies on crystalline aquifers considering only vertical flow paths. Reactivity in saprolite or in horizontal less-weathered fractures may be different. Information on temporal evolution and change with depth of the geochemical features of water is almost not available in this context, as studies mainly rely on single-date measurements (a single pumping event, logging on a single date, discrete water sampling). To date, little is known about (1) the spatial evolution of the flow paths with depth and (2) flow-path dependence on the water level variation and, consequently, its temporal evolution during recharge events.

The current report proposes to fill this gap and presents a conceptual model of recharge in weathered crystalline aquifers based on detailed field investigations. To do so, this work uses a percolation tank as a practical tool to deal with the dynamics of indirect recharge processes. Its monitoring provides a strong and easily identifiable surface-water input signal (i.e. recharge tracer) in the aquifer. The purpose here is not to quantify the recharge efficiency of a water tank, which has been previously done on this specific site (Boisson et al. 2014).

The aim of the present study is to describe the mechanisms and dynamics of recharge in crystalline aquifers at a local scale, in correlation with MAR structures. A range of methods were used, including the use of a borehole camera, drilling cuttings, vertical flowmetry, water electrical conductivity (EC) logging, water quality analyses (major ions, ^{18}O and ^{2}H) and water level monitoring. These complementary methods, ran over one hydrological year, provide a unique data set. The study addresses local recharge mechanisms and their temporal evolution and discusses their impact on water quality, MAR monitoring and assessment methodologies.

Study site

The study was conducted at the artificial recharge site of the Tumulur tank, located in Maheshwaram watershed, 35 km from the city of Hyderabad (Telangana State; Fig. 1). The Maheshwaram watershed has been described in several studies (e.g. Dewandel et al. 2006; Maréchal et al. 2004, 2006). This watershed is typical of the South Indian semi-arid context: heterogeneous weathered hard-rock aquifer, irrigated agriculture dominated by paddy fields, heavy groundwater withdrawal and solute recycling issues (Perrin et al. 2011a, b; Pettenati et al. 2013). The annual rainfall measured in Hyderabad (ICRISAT meteorological station) over the 1974–2013 period was 870 mm, with a minimum of 530 mm in 1985 and 2011, and a maximum of 1,450 mm reached in 2000. Precipitation occurs mainly during the highly variable monsoon period. The potential annual evapotranspiration is 1,800 mm.

The bedrock of the catchment is mainly biotite, granites and leucocratic granites with some quartz veins and dolerite dykes (Fig. 1). The local weathering profile at the Tumulur area is typical of crystalline aquifers, usually defined from top to bottom (Fig. 2) by (1) a saprolite layer a few tens of meters thick (also called regolith), (2) the fractured layer and (3) the fresh bedrock. The saprolite is derived from bedrock decomposition (Acworth 1987; Chilton and Foster 1995; Dewandel et al. 2006). Given its clayey–sandy composition, the saprolite has a high porosity but a relatively low permeability and

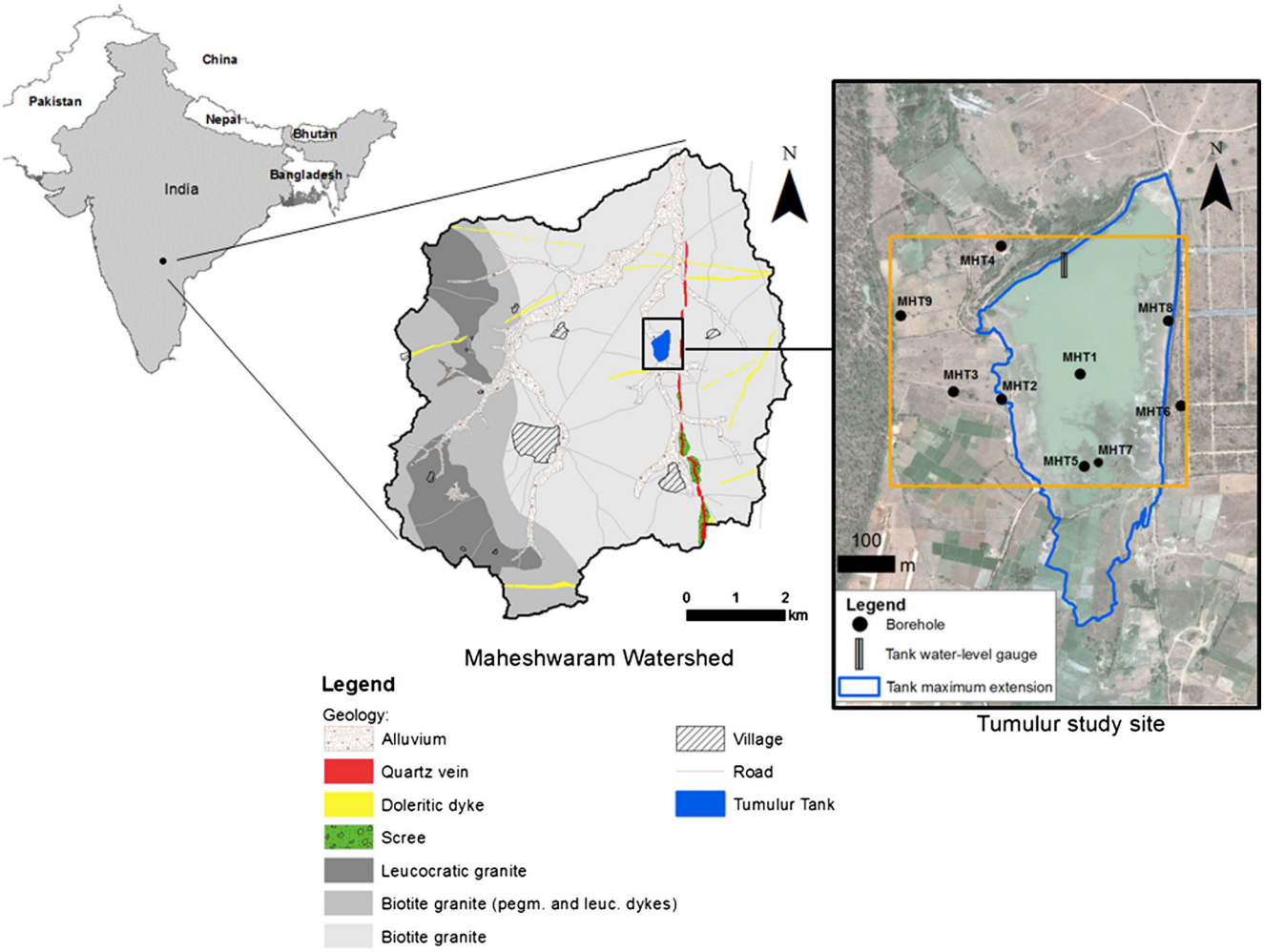

Fig. 1 Maheshwaram watershed geology and Tumulur tank study site, with spatial extension of the tank, as measured on four occasions during the 2013 monsoon. The location of the electrical conductivity maps discussed later in the report is represented by the *yellow rectangle*

represents the main groundwater stock of the aquifer when saturated (White et al. 2001; Wyns et al. 2004). Within this layer, a few preserved conductive fractures may exist, creating preferential flow paths. Below the saprolite, the fractured layer constitutes the main transmissive zone of the aquifer, due to its subhorizontal and subvertical fissures network. It is tapped by most of the wells drilled in hard-rock areas.

The monitored tank (Fig. 1) is made of an earth bund which dams the natural ephemeral stream outlet and consequently stores runoff water. Its maximum capacity is about 4 m depth corresponding to 130,000 m^2. It is regularly empty during the dry season. No direct tank-water extraction for irrigation occurs but at least 15 irrigation wells extract groundwater within 1 km^2 around the tank, mainly for rice field irrigation. The current tank system can be considered as a representative example of MAR practices in semi-arid southern India. More details on the tank functioning and efficiency can be found in Boisson et al. (2014). Seven boreholes (MHT1, MH2, MHT3, MHT4, MHT5, MHT8 and MHT9) were drilled in 2012 in a 0.3 km^2 area around the percolation tank, and were solely used as observation sites (Fig. 1). The casings were cemented to avoid surface-water bypass.

Methodology

The local weathering profile in the Tumulur area based on data from geological logs and ERT (electrical resistivity tomography) profiles shows a deepening of the profile from north to south (Boisson et al. 2014). Conductive-fracture locations and flow were assessed using heat-pulse flowmeter (HPFM) measurements (Paillet 1998) carried out for ambient flows and under pumping conditions in the MHT2, MHT3 and MHT5 boreholes in April and May 2014. Ambient conditions allow for measurement of natural flow upward and downward between fractures under different hydraulic head conditions.

Water electrical conductivity (EC) profiles in the boreholes were assessed through eight logging campaigns using an OTT multi-parameters probe (measurement precision±1 μS/cm) between May 2013 and April 2014. EC profiles reflect the

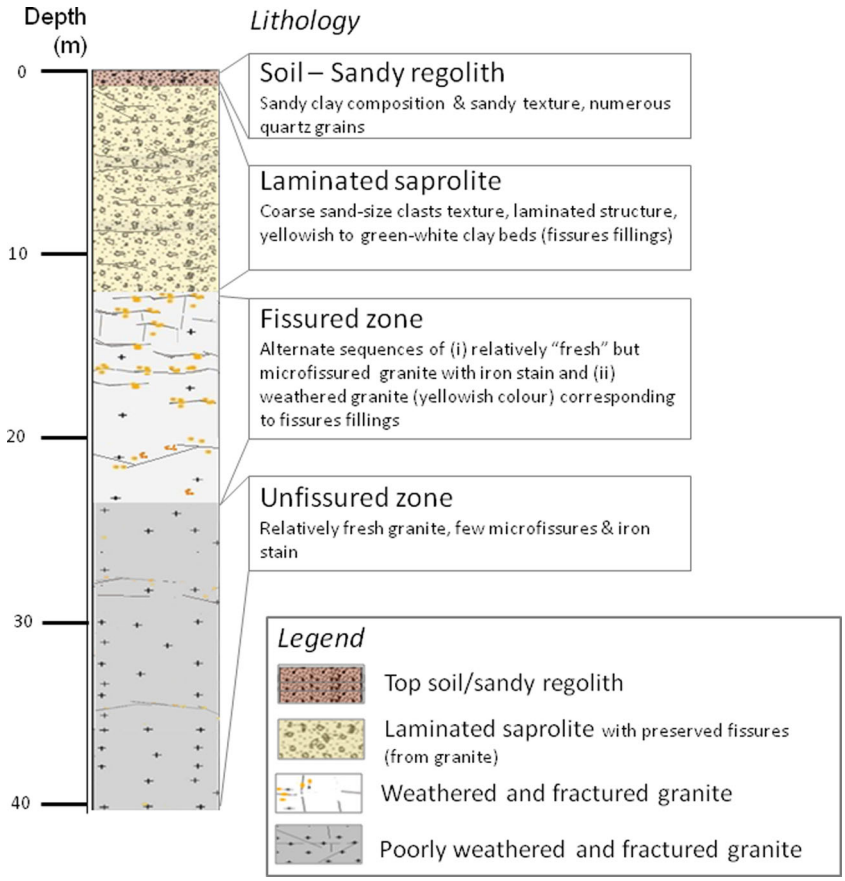

Fig. 2 Typical geological log

ambient conditions in equilibrium with the surrounding fluids (Boutt et al. 2010). Steep changes in EC profiles indicate halocline and/or location of flowing fractures; hence, EC profiles give valuable information on conductive-fracture locations and have been used for the calculation of conductive fractures density in the seven boreholes.

Two slug test campaigns, conducted in May 2013 (dry period) and in March 2014 (high groundwater levels and high water level in the tank), allowed estimation of the local hydraulic conductivities of the boreholes during contrasted hydrologic conditions. The aquifer thickness was assessed thanks to the geological logs of the boreholes coupled with camera observations allowing the determination of the thickness of the fractured zone in each borehole. The different hydrological conditions for similar periods occurred due to monsoons with contrasted intensities (<700 mm in 2012 and more than 1,100 mm in 2013). Slug tests were interpreted using the Bouwer and Rice method (Bouwer and Rice 1976). Data loggers recording water level at 15-min intervals were used in the tank and in the seven boreholes. In addition, global positioning system (GPS) tracking was performed twice a month to assess the evolution of the water surface of the tank. As for many studies in semi-arid environments, the Maheshwaram watershed undergoes strong environmental heterogeneities, both spatial and temporal (e.g. erratic rainfall, discontinuities of the surface water repartition), regarding the available data. Because the Tumulur tank gathers runoff water from the small catchment, the recorded water levels of the Tumulur tank provide valuable information on the hydrological conditions over the study area. Data acquisitions were run between January 2013 and April 2014.

Water chemistry was determined based on five sampling campaigns between February 2013 and February 2014 in the seven boreholes and the Tumulur tank. A total of 28 groundwater samples and 5 surface-water samples were collected for major ions analyses. Isotopic analyses ($\delta^{18}O$, $\delta^{2}H$) were run on 37 groundwater and 4 surface-water samples. Groundwater samples were collected after 30 min of pumping in the borehole, allowing the extraction of 3 times the volume of the wells, except for MHT8 for which water is not renewed. In order to assess the vertical heterogeneity, for one campaign in February 2014, the boreholes were sampled at two depths for each borehole with a point-source bailer. During the 2013 monsoon, cumulative rainfall of August, September and October 2013 were sampled at the Maheshwaram meteorological station for $\delta^{18}O$ and $\delta^{2}H$ analyses. An ICP-emission spectrometry method, ionic chromatography and mass spectrometry were used for the analyses of cations, anions and the stable isotopes, respectively. Potentiometric titrations were performed to assess the alkalinity. Hydrodynamic data (e.g.

piezometry, surface-water levels, transmissivities) and stable isotope data of the water in the tank and in the boreholes were collected to represent very contrasted hydrological situations, ranging from high water levels (November 2013, February 2014) to low-water-level conditions (February 2013).

Results and interpretation

Water level variations in response to recharge

Water level evolution in the tank and the observation wells is provided in Fig. 3. From January 2013 to June 2013, the percolation tank remained dry. The tank filled rapidly in response to strong rain events and emptied slowly through infiltration and evaporation. While the infiltration rate was relatively stable over the year (~4.5 mm/day; Boisson et al. 2014), evaporation intensity varied from 3.5 to 12 mm/year.

In 2013, four major rain events filled the tank from June to October 2013 (Fig. 3). The last event led to the maximum possible height reached in the tank (around 3.8 m above ground surface; Figs. 1 and 3a). Two stages of the monsoon can be defined: the first stage between June and September 2013 for which the rainfall amount is relatively low and the surface-water levels were moderately high (depth of the tank <2 m) and the second stage that lasted from the strong event on 24 October 2013 to April 2014 when the tank area reached its maximum and then decreased (Figs. 3 and 4).

Hydrodynamics of the aquifer are closely linked to the dynamics of the tank reservoir (Fig. 3b,c). Rising of the tank level after a flood is quickly followed by a rise of groundwater level. Most of the boreholes exhibited fast and strong responses (water levels in MHT1, MHT2, MHT3, MHT5 and MHT9 rose within the same day of the rain event), while others presented slower responses (i.e. MHT8; 2 days later). The monitored piezometric signals are under the influence of

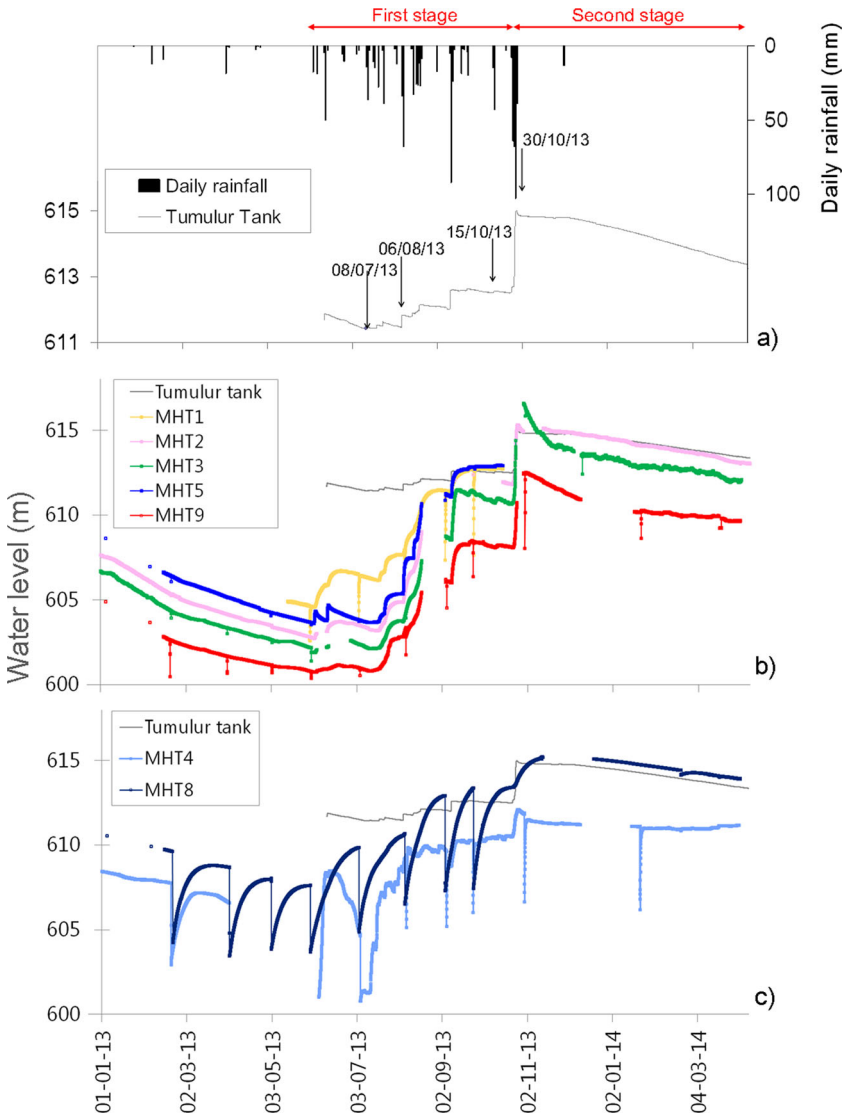

Fig. 3 **a** Daily rainfall from 1 Jan 2013 to 3 April 2014 and the Tumulur Tank surface-water elevation—meters above mean sea level (m a.m.s.l.)—with the dates corresponding to the tank area drawn on Fig. 1. The first and the second monsoon stages are indicated. **b** Hourly piezometric levels in boreholes *MHT1*, *MHT2*, *MHT3*, *MHT5* and *MHT9*. **c** Hourly piezometric levels in boreholes *MHT4* and *MHT8*. The water levels in boreholes MHT1 and MH5 are not presented after the rain event (i.e. 23 October 2013) since these boreholes were flooded and the data loggers were damaged. The surface-water level is missing for the first filling-up event in June 2013. Sudden water level drops are due to pumping for water sampling

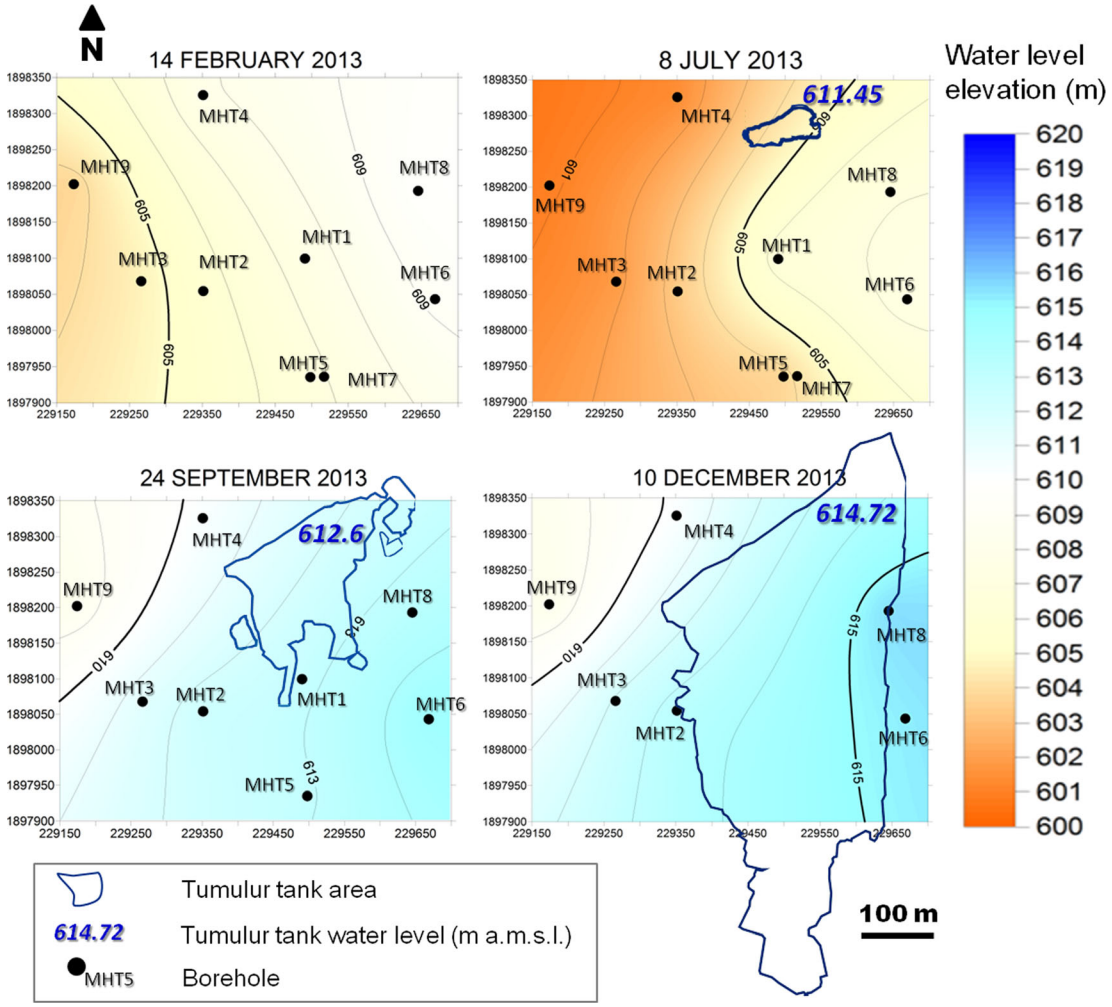

Fig. 4 Piezometric maps for *February*, *July*, *September* and *December* 2013 with the corresponding tank surface (kriging interpolation)

the monthly pumping conducted for water sampling which variously impacted the piezometry of the MHT wells (sudden drops on Fig. 3b,c).

The significant difference in amplitude and reactivity between the boreholes clearly marks the heterogeneity of flows in the fractured granite. Note that the amplitudes of the rise of water levels in the boreholes are not linearly correlated with the rainfall intensity. When the water levels are low (i.e. at the bottom of the fractured zone) a small rainfall event can induce an important rise of water level. On the other hand, under high-water-level conditions, important rainfall events induce negligible rises in water levels (Fig. 3) due to a higher porosity of the upper part of the profile (saprolite), as described in Fig. 2.

Changes in transmissivity with depth were assessed through two slug-test campaigns during different water level conditions (Table 1). Computed transmissivities range from 1.8×10^{-4} to 3.7×10^{-7} m^2/s in 2013 (low water levels) and from 1.3×10^{-3} to 5.1×10^{-6} m^2/s in 2014 (high water levels). During the high-water-level period, transmissivities are on average 8 times higher than during the low water period, except for MHT3. The varied transmissivities (Table 1) explain the contrasted responses of the wells to the monthly pumping for sampling. As an example, for MHT4 in February 2013 (a low water period) the recovery rate was about 0.2 cm/h over 20 days, while it reached 16 cm/h and lasted only 30 h in August 2013 (a high-water-level period).

Pumping tests in MHT8 could not been run properly because of the important drawdown and the very long recovery time. Water levels of MHT8 are disturbed for tens of days after sampling, which implies a very low transmissivity (although actual transmissivity is not known). MHT2 well (high transmissivity) does not show any impact at hourly intervals (Fig. 3).

Hydraulic gradients between wells are variable depending on the hydrologic conditions. The gradient direction between MHT4 and other wells (MHT1, MHT2, MHT3 and MHT5) reversed between low water levels (i.e. February 2013) and high water levels. Initially, groundwater flowed toward the south-west, while later it flowed to the north-west (Figs. 3 and 4).

Some boreholes presented water levels higher than the tank and soil level for a while (MHT2, MHT3 and MHT8 on Fig. 3) despite being close to it. This indicates a locally confined behavior, at least for a short period and highlights a lack

Table 1 Borehole elevation, depth and slug test results for the April 2013 (low water level) and March 2014 (high water level) campaigns. (*NA* not available, *K* hydraulic conductivity)

Borehole	Elevation (m a.m.s.l.)	Borehole depth (m)	2013 campaign				2014 campaign				Differences	
			Average K (m/s) Boisson et al. 2014	Depth to water table (m)	Considered aquifer thickness	Transmissivity T (m^2/s)	Average K (m/s) Boisson et al. 2014	Depth to water table (m)	Considered aquifer thickness	Transmissivity T (m^2/s)	Δ WL (m)	Increase factor of T
MHT1	613.28	NA	NA	NA	NA	NA	NA	NA	NA	NA	NA	NA
MHT2	615.06	77.7	2.5×10^{-6}	5.45	72.3	1.8×10^{-4}	1.7×10^{-5}	1.68	76.0	1.3×10^{-3}	3.77	7.3
MHT3	617.36	51	1.3×10^{-6}	15.5	35.5	4.6×10^{-5}	1.0×10^{-6}	5.31	45.7	4.6×10^{-5}	10.19	1.0
MHT4	613.19	32	2.4×10^{-8}	16.3	15.7	3.7×10^{-7}	1.7×10^{-7}	2	30.0	5.1×10^{-6}	14.3	13.6
MHT5	614.13	88.3	5.4×10^{-7}	5.78	82.5	4.5×10^{-5}	3.8×10^{-6}	0.56	87.7	3.3×10^{-4}	5.22	7.5
MHT8	615.32	50	NA	NA	NA	NA	NA	NA	NA	NA	NA	NA
MHT9	616.33	60	8.4×10^{-7}	16.13	43.9	3.7×10^{-5}	2.0×10^{-6}	2	58	1.2×10^{-4}	14.13	3.1

of major vertical connectivity and/or a low vertical permeability.

Water level monitoring and slug tests highlight (1) a strong correlation between water level evolution and tank water-level evolution; (2) a heterogeneity of boreholes' reaction to recharge with both steep and smooth rising of water levels; (3) a decrease of the hydraulic gradients between the boreholes during high water level; (4) a decrease of transmissivity and porosity with depth (non-linearity of the borehole response) due to the decreasing degree of the weathering with depth and the structure of the fissure network; (5) a low vertical connectivity or a confined behavior as highlighted by some artesian boreholes.

Fractured zone structure and recharge dynamics

To assess the flow path within the aquifer, a comparison of geological logs, electrical conductivity (EC) logging, vertical flowmetry (under ambient and pumping conditions) and borehole camera observations was performed in each borehole. An example is presented for MHT5 in Fig. 5. Despite a large number of fractures observed in MHT5 with the borehole camera and the numerous marks of alteration during drilling (Fig. 5a, d), just a few discrete fractures (2–3) appeared to conduct most of the flow, as noted by a sharp increase of flow rates in the flowmetry measurements (Fig. 5c). Under ambient conditions, in May 2014 (high water level), natural vertical upward flows within the borehole (65–55 and 40–30 m) highlight the presence of fractures intercepting compartments with different hydraulic heads identified as F1, F2 and F3 in Fig. 5c. Ambient upward flow indicates that fractures in the deeper part of the borehole have a higher hydraulic head than the shallow fractures and that fractures are vertically disconnected. This vertical disconnection highlighted by ambient upward flows was also observed in boreholes MHT2 and MHT3 (not shown).

HPFM measurements under pumping conditions indicate that only two of the three fractures previously identified are significantly conductive: F1 and F2 located at depths of 30 and 55 m. There is also a major increase of the flow close to the cased section (Fig. 5a,c).

EC profiles indicate a high variability of electrical conductivity in depth and time (Fig. 5b). Depending on measurement time, stratification in the well is more or less marked. The different EC profiles performed show a good match between the conductivity breakpoints (sharp change of the EC) and the conductive fractures (Fig. 5b,c).

A comparative analysis of borehole camera observations and breakpoints in EC profiles was performed in each borehole in order to determine the main conductive fractures. It was then possible to assess the conductive-fractures density (CFD) with depth for the seven boreholes (shown in Fig. 6). Data were homogenized by calculating depth below the saprolite, since the upper sections of the boreholes (saprolite) are cased.

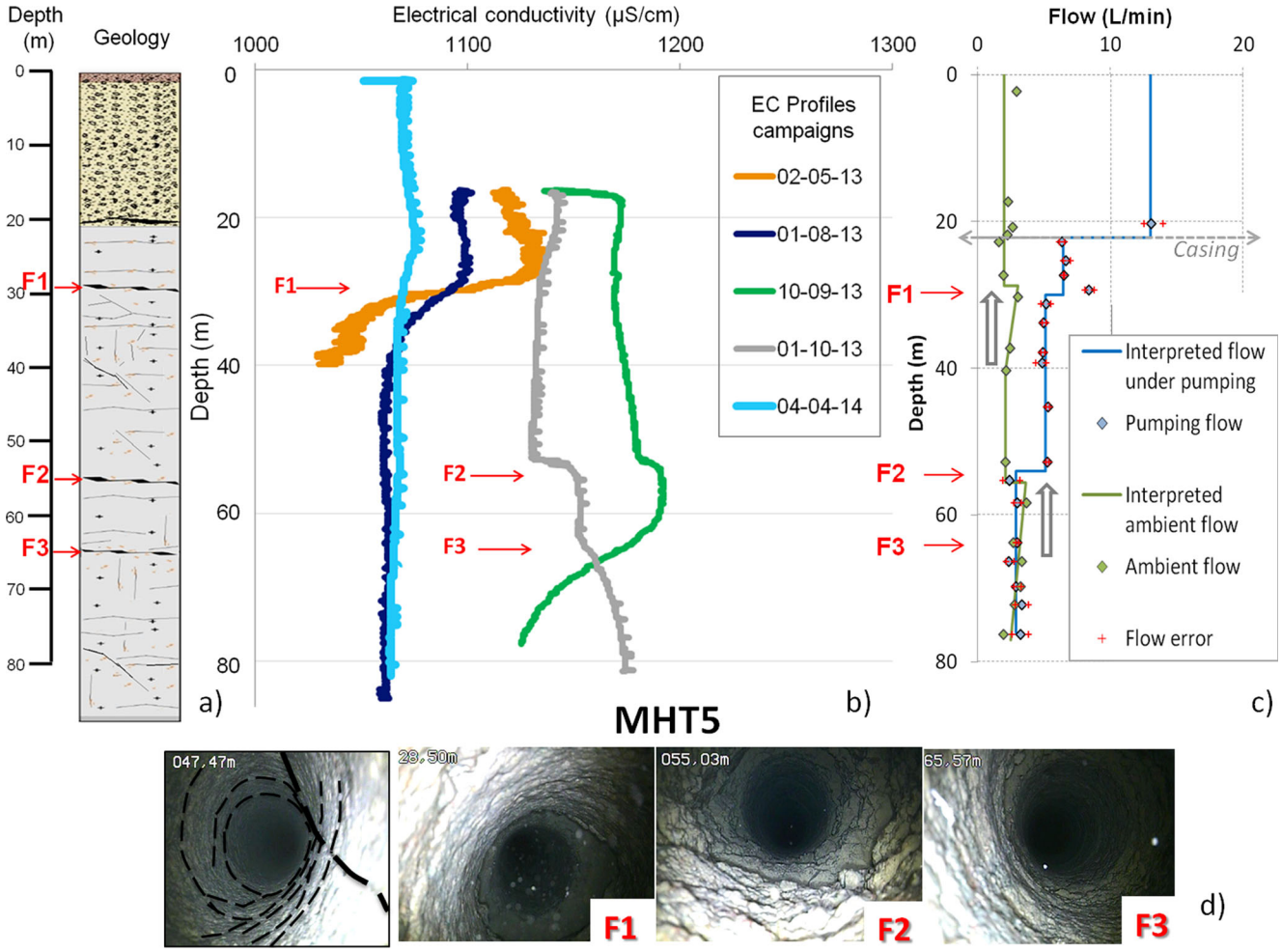

Fig. 5 **a** Geological log, **b** electrical conductivity (*EC*) profiles (May, August, September, October 2013 and April 2014) and **c** heat-pulse flowmeter (HPFM) results in borehole *MHT5*. **d** From *left to right*: Borehole camera pictures of the fissured zone and three productive fractures identified based on the log data

Measurement density is maximal down to 15–20 m depth then decreases as a function of borehole length. Beyond 55 m below the saprolite, the measurement density (two boreholes) is not considered representative of the crystalline aquifer. The density of conductive fractures decreases with depth. Most of the conductive fractures are located in the top of the fissured layer. Beyond 20 m below the saprolite (i.e. about 35 m below the ground level), there is a significant decrease of the number of conductive fractures.

Note that the use of EC breakpoints allows location of the conductive fractures but does not provide information on their relative contribution to the total flow, as is feasible with the HPFM measurements. The use of HPFM in the most transmissive boreholes (MHT2, MHT3 and MHT5) shows that a limited number of discrete conductive fractures (3–4) provides most of the flow within the borehole (Fig. 6c).

Comparison of EC profiles (Fig. 7) in all boreholes at different dates shows that EC varies from 500 to 3,500 µS/cm, with strong horizontal and vertical heterogeneities evolving with time. Surprisingly, EC of MHT1 is significantly higher than the other boreholes (>2,000 µS/cm) despite its location in the middle of the tank (Fig. 1).

In May 2013, when there was no influence from the recharge, EC was variable horizontally as well as vertically (Fig. 7). Once the tank is flooded (after June 2013), the water columns within the boreholes are stratified. The EC concentrations are globally higher in the deepest part of the boreholes and, apart from MHT1, are close (i.e. EC between 1,000 and 1,300 µS/cm below 580 m). The increase in the number of breakpoints along several borehole profiles (i.e. the stratification of the water column) may come from the contribution of newly active fractures. The contribution of the fractures toward the water stratification seems to evolve with time.

The presence of breakpoints in EC profiles, coupled with the presence of vertical ambient flow confirm that the boreholes cross fractures intercepting disconnected compartments with variable hydraulic heads and chemistry. The changes in

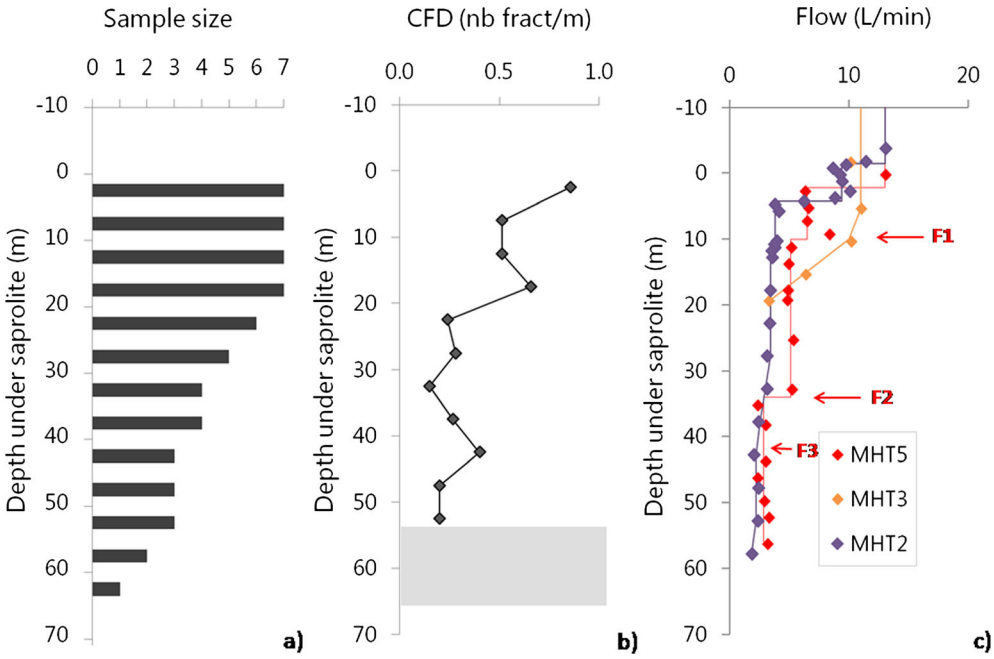

Fig. 6 **a** Sample size (number of observed boreholes) and **b** conductive-fractures density (*CFD*) below the base of the saprolite for all boreholes, presented as the number of fractures per meter (*nb fract/m*) for 5-m intervals. *Grey colour* indicates the section where data are considered to be non-representative (sample size <2 boreholes). **c** HPFM measurements under pumping condition for the most transmissive boreholes (*MHT2*, *MHT3* and *MHT5*). The locations of the fissures *F1*, *F2* and *F3* are drawn

breakpoint locations also point out the temporal evolution of the hydraulic heads and the conductive fractures activations.

To assess these spatial and temporal dynamics, for all boreholes, the breakpoint elevations in EC profiles have been compiled in Fig. 8, neglecting the EC values. Before the monsoon season (i.e. May 2013, Fig. 8a) most of the EC profiles were homogeneous; therefore breakpoints were rare. With the monsoon arrival—June and after (Fig. 8b–f)—the number of

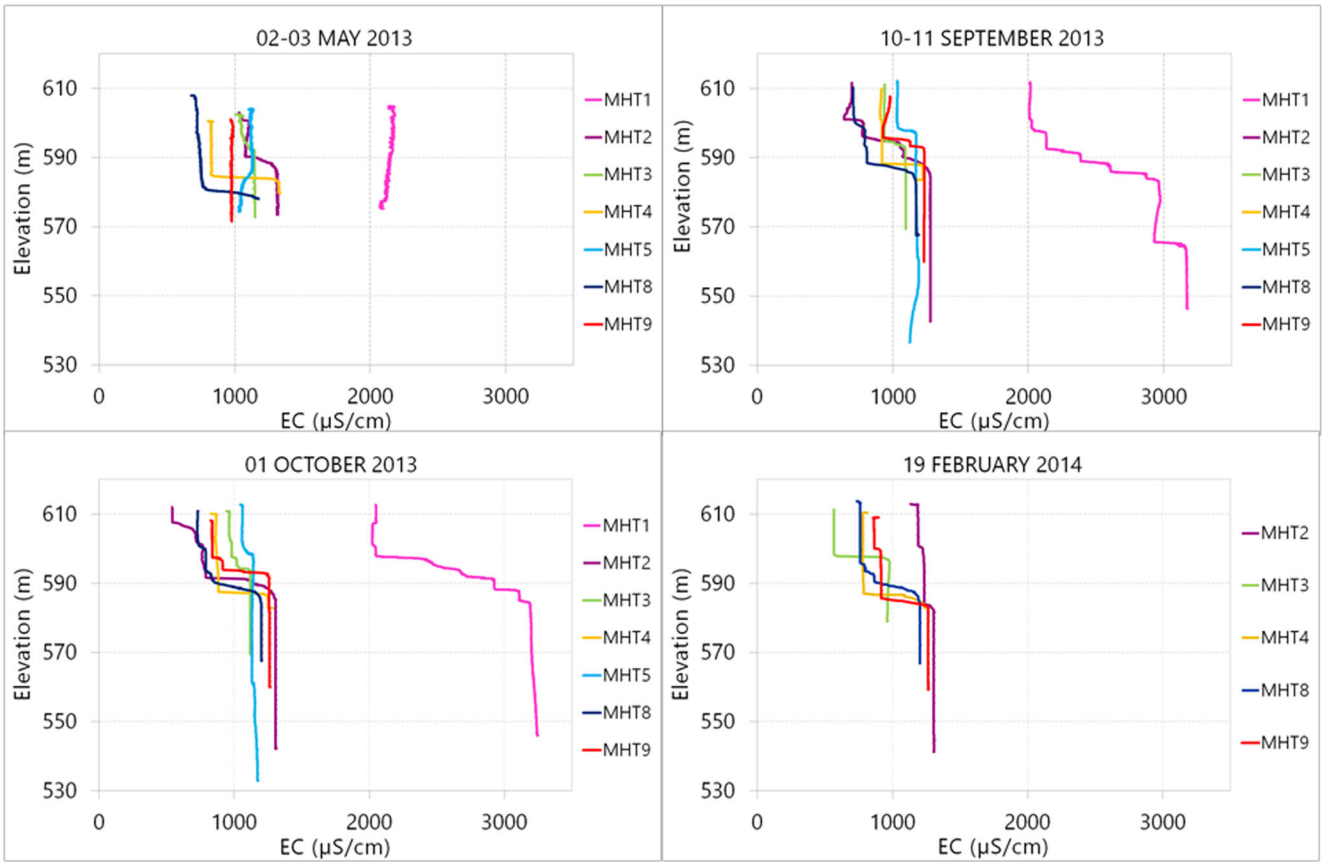

Fig. 7 EC profiles for the *May 2013*, *September 2013*, *October 2013* and *February 2014* campaigns

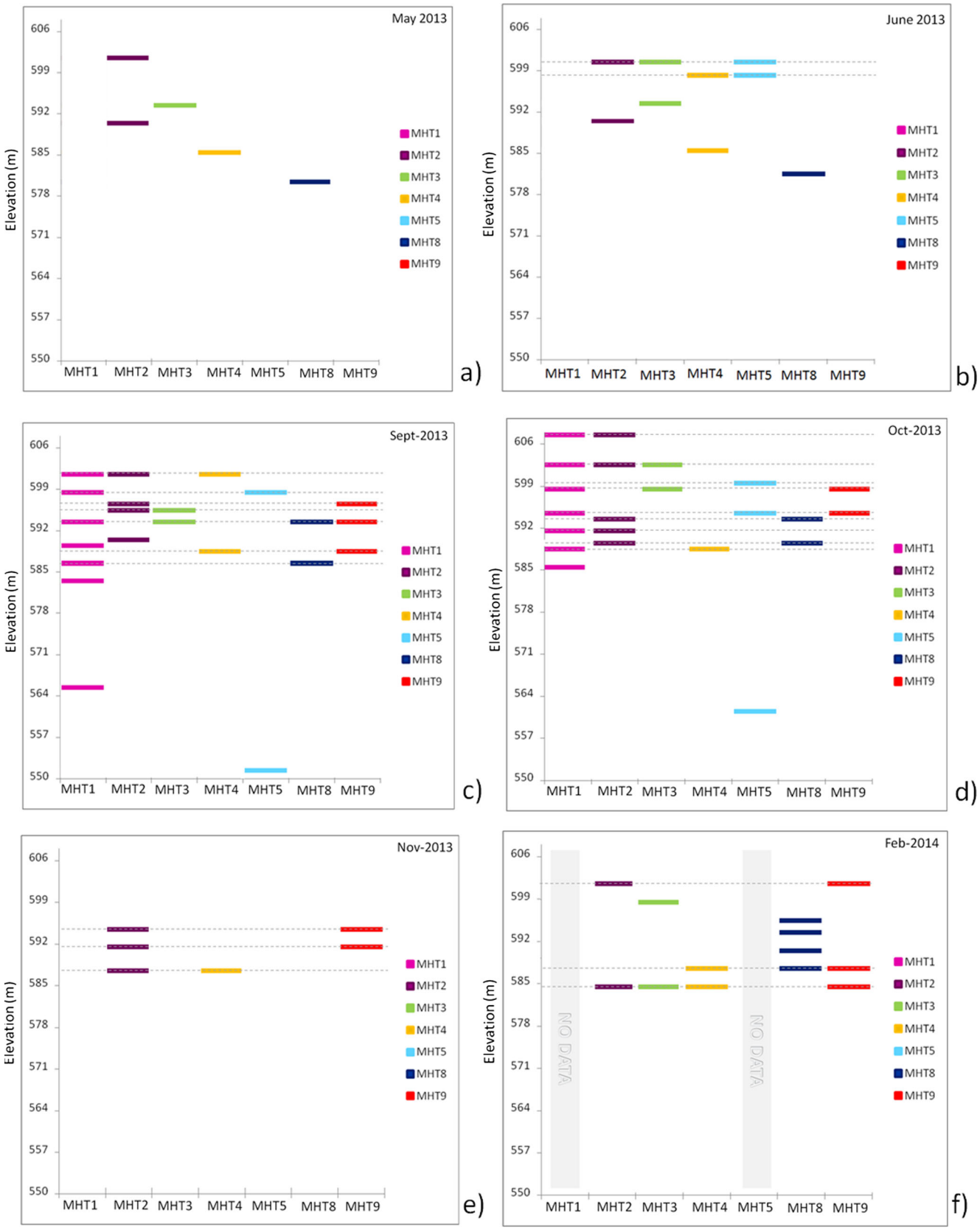

Fig. 8 Elevations of the breakpoints in the EC profiles of the boreholes for the *May*, *June*, *September* and *November* 2013 and *February* 2014 campaigns. For each borehole, the breakpoints are indicated by *horizontal bars* at the corresponding elevation. *Dotted lines* are drawn where at least two breakpoints are located at the same elevation

breakpoints increased in each borehole. There was a clear convergence of breakpoint elevations in the different borehole profiles. None of the breakpoint elevations in EC profiles were similar in May, while in October 2013, most of the breakpoint elevations were similar for several boreholes, which highlights the stratification of the water column and the increase of horizontal connectivity with rising water levels. The most important breakpoints were located in the upper part of the boreholes, i.e. about 90 % were located between 580 and 600 m; however, a few deep EC breakpoints show the occurrences of relatively deep water circulation—e.g. MHT5 in September and October showed breakpoints located at 551 and 561 m respectively (Fig. 8c,d). The deep breakpoints are unique and indicate a limited connectivity of the fracture network in space.

The evolution of these connections, highlighting the evolution of the horizontal connectivity with water level and the large extension of the upper fracture network, can be schematized along the hydrologic year as shown on Fig. 9. The deepest parts of the boreholes which show isolated breakpoints remain the inactive part of the aquifer.

Mapping the evolution of the EC between May and September 2013 (i.e. before and after heavy rainfall events) for different depth ranges (0–5, 10–15, 15–20 and 25–30 m below the saprolite base) allows one to see that the EC variations are very heterogeneous in space, with no clear trend in the spatial repartition (Fig. 10). This representation shows that the dilution from the tank and rainfall water was limited to a few meters and a few boreholes (MHT2 and MHT3), while the increase of EC in the deeper parts of the borehole showed an inflow from the deepest fractures. Note that MHT1 borehole, located in the centre of the tank, does not seem to be impacted by the water from the tank, as there is no observable dilution. On the hand, the increase of EC in MHT1 from 25 to 30 m below the saprolite indicates a deep horizontal flow, disconnected from the close surface.

A relevant example of the influence of the deep horizontal flow is that the water level in MHT8 rose 9.3 m from the initial level during the recharge period. Within the borehole, the halocline also rose 9.3 m from the initial level in the same time. It seems to show that the rise in this borehole was due to a rise from a deep part of the water column through horizontal flow, despite being located a few meters from the percolation tank (or even flooded for a while). Hence, no direct vertical flow seemed to impact the water level variation in this borehole.

In summary, the HPFM measurements coupled with the electrical conductivity profiles at different dates provide the following information on recharge dynamics at local scale: (1) a few horizontal fractures, mostly located at the top of the profile, appear to control the flow; (2) hydraulic heads of the different compartments intercepted by horizontal fractures appear to be different and connectivity between them is evolving with time; (3) horizontal connectivity increases with the rise of water level; (4) the aquifer is very stratified chemically; (5) horizontal flow

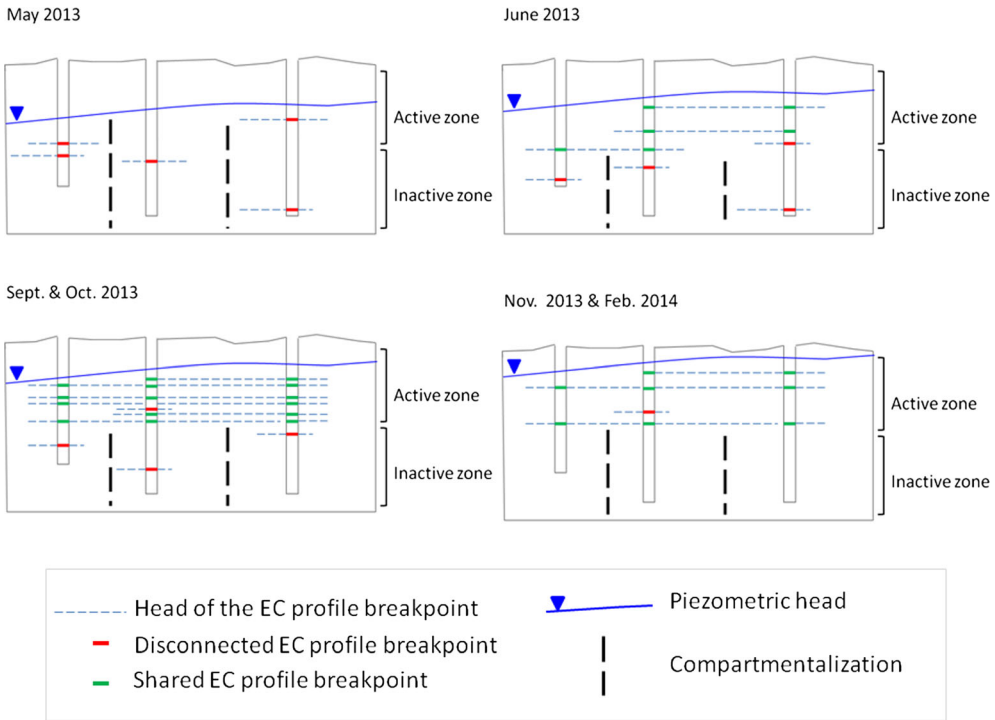

Fig. 9 Schematization of the evolution of the connectivities among the EC profile breakpoints within the weathered crystalline aquifer along the hydrologic year

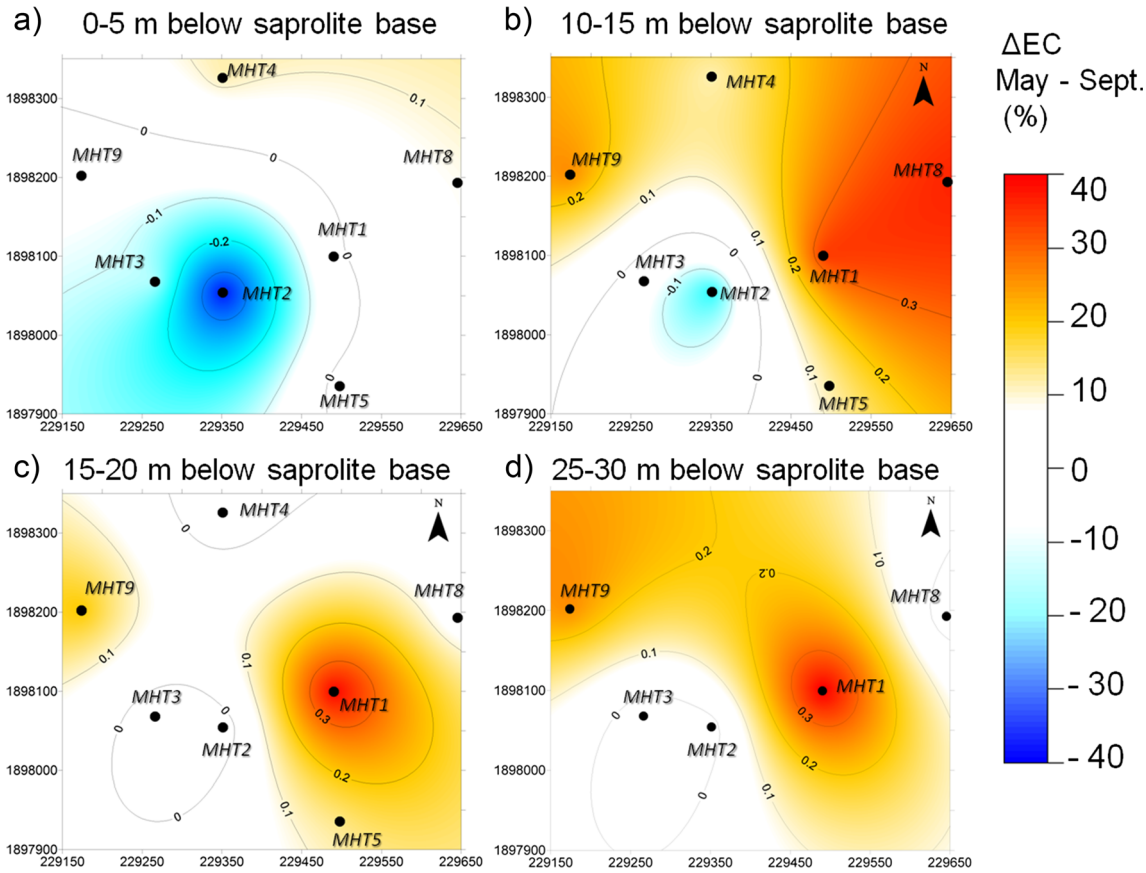

Fig. 10 Maps (kriging interpolation) of the EC changes between May 2013 and September 2013 (in %) between **a** 0 and 5 m, **b** 10 and 15 m, **c** 15 and 20 m and **d** 25 and 30 m below the saprolite base. The location of the maps is represented by the yellow rectangle in Fig. 1

appears to have a major impact on water level changes within the wells, highlighting a piston-flow/preferential-flow-path recharge pattern, (6) direct vertical infiltration does not appear to be the main pattern.

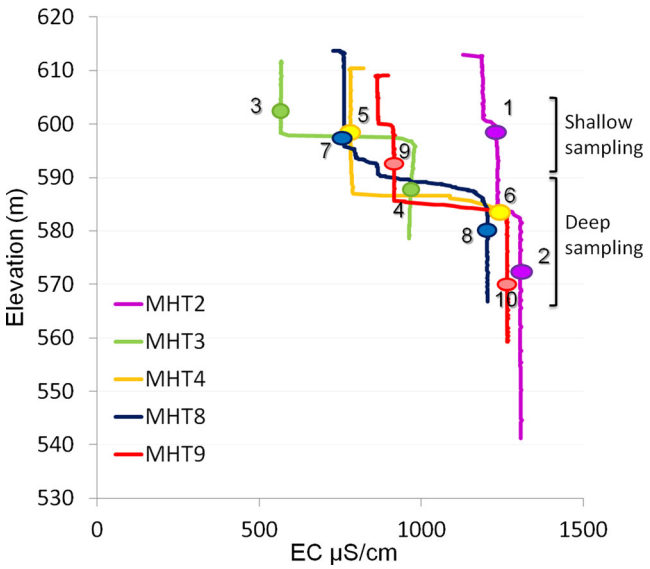

Fig. 11 EC profiles of the February 2014 campaign; sampling points for the isotopic and major ions analyses (ID numbers *1–10*) are listed in Table 2

Groundwater quality and chemical heterogeneity

Major ion and isotope analyses are compared for February 2013 (i.e. dry period: equilibrium state before recharge), September and November 2013, and February 2014 (i.e. high water levels) campaigns. During the February 2014 campaign, samples were taken at different depths (see Fig. 11 and Table 2 for sampling depths).

Table 2 Identification, depth of sampling and electrical conductivity value of the February 2014 samples in Figs. 11, 12c and 13. *ID* Identification numbers

ID	Borehole	Sampling depth (m)	EC (µS/cm)
1	MHT2	15	1,230
2	MHT2	40	1,305
3	MHT3	15	567
4	MHT3	30	975
5	MHT4	13	780
6	MHT4	30	1,200
7	MHT8	18	762
8	MHT8	35	1,200
9	MHT9	23	915
10	MHT9	40	1,260

Groundwater quality during dry period

The $\delta^{18}O$ of the groundwater in February 2013, plotted versus $\delta^{2}H$ (expressed in ‰ vs. Standard Mean Ocean Water, SMOW), line up on an evaporation line that intercepts the local meteoric water line (LMWL) at −4.4 and −26 ‰ values, for $\delta^{18}O$ and $\delta^{2}H$, respectively (dark blue dots on Fig. 12). The LMWL is very close to the global meteoric water line (GMWL) and was defined by Kumar et al. (2010) for South India as $\delta^{2}H=7.82$ (±0.17)×$\delta^{18}O+10.23$ (±0.85) ‰ vs. SMOW. The evaporation line has a slope of 4.2. The range of groundwater isotopic facies is large. MHT1 has the least evaporated facies and MHT4 the most evaporated (Table 3).It is noteworthy that the water facies of MHT1 and MHT8 are very different from the other boreholes, and also different from the tank, despite being very close to it and often flooded: the dominant chemical facies of the groundwater is neutral to HCO_3–Na, but MHT1 has a Ca–Cl facies and MHT8 has a strong HCO_3–Na facies (Fig. 13).

Surface-water quality

The isotopic content of rainfall in 2013 varied from −13.6 to −2.1 ‰ for $\delta^{18}O$ and from −99.3 to −9.2 ‰ for $\delta^{2}H$ along the LMWL (not shown). Surface water (SW) appeared in June 2013 and lasted to June 2014 and beyond. Its isotopic signature was highly variable in time, depending on rainfall events (signature and amount) and evaporation processes. It was close to the groundwater contents in September 2013 (Fig. 12). As a result of the strong rain event of 24 October 2013 ($\delta^{18}O=-13.6$ and $\delta^{2}H=-99.3$ ‰ vs. SMOW, not

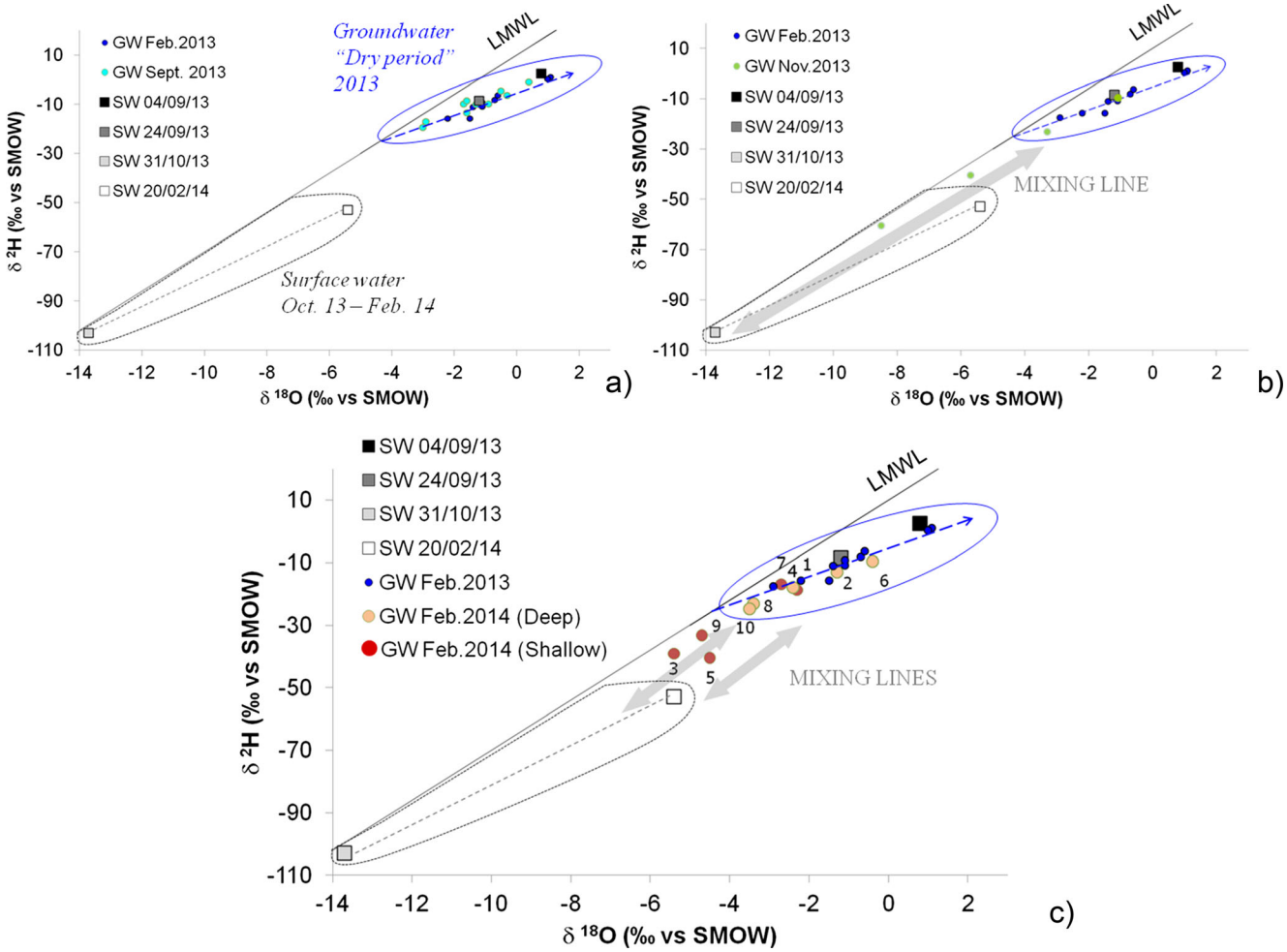

Fig. 12 $\delta^{18}O$ vs $\delta^{2}H$ of groundwater (*GW*, *dots*) during the "dry period" (i.e. February 2013) compared to other periods and surface water (*SW*, *squares*) sampled on 4 September 2013, 24 September 2013, 31 October 2013 (i.e. after the strong rain event of 24 October) and 20 February 2014, at the Tumulur study site. The isotopic signature of the depleted surface water post-October-2013 is surrounded with a *grey dotted line* and the groundwater "dry period" pole is surrounded by the *blue line*. *LMWL* is the local meteoric water line. Groundwater and surface water mixing lines are represented by the *grey arrows*. **a** Comparison of the isotopic signatures of the groundwater of the February 2013 (i.e. "dry period", *dark blue dots*) and September 2013 (i.e. early stage of the monsoon, *light blue dots*) samples; **b** Comparison of the February 2013 and November 2013 samples—i.e. late stage of the monsoon (after the strong rain event), *light green dots*; **c** Comparison of the February 2013 and February 2014 (i.e. late stage of the monsoon) samples. Deep samples of February 2014 campaign are *light orange dots* and shallow samples are *red dots*. ID numbers of the samples (Table 2) are indicated

Table 3 Isotopic contents (‰ vs. SMOW) of the groundwater samples for the pre-monsoon (February 2013) and post-monsoon (September 2013, November 2013 and February 2014) campaigns. The identification (*ID*) numbers of the February 2014 samples in Figs. 11, 12 and 13 are indicated. *NA* not available; *ID* identification number

Borehole	Pre-monsoon		Post-monsoon							
			First stage		Second stage					
	Feb 13		Sep 13		Nov 13		Feb 14			
	$\delta^{18}O$	$\delta^{2}H$	$\delta^{18}O$	$\delta^{2}H$	$\delta^{18}O$	$\delta^{2}H$	Sample depth	$\delta^{18}O$	$\delta^{2}H$	ID
MHT1	−2.9	−17.6	−3	−19.3	NA	NA	MHT1	NA	NA	–
MHT2	−0.6	−6.3	−1.7	−9.7	−1.2	−9.4	MHT2: 15 m	−2.3	−18.7	1
							MHT2: 40 m	−1.3	−13	2
MHT3	−1.1	−9.2	−1.3	−9.9	−8.5	−60.6	MHT3: 15 m	−5.4	−39.1	3
							MHT3: 30 m	−2.4	−17.9	4
MHT4	1	0.4	−0.5	−4.5	−3.3	−23.3	MHT4: 13 m	−4.5	−40.4	5
							MHT4: 30 m	−0.4	−9.6	6
MHT5	−1.4	−11.1	−1.6	−13.4	NA	NA	MHT5	NA	NA	–
MHT8	−2.2	−15.8	−2.9	−16.9	NA	NA	MHT8: 18 m	−2.7	−16.9	7
							MHT8: 35 m	−3.4	−23.2	8
MHT9	−1.5	−15.7	−1.6	−8.5	−5.7	−40.5	MHT9: 23 m	−4.7	−33.2	9
							MHT9: 40 m	−3.5	−24.8	10

shown), surface water sampled on 31 October was very depleted. As no more significant input occurred in the tank, the isotopic signature of the surface water sampled in February 2014 resulted from the evaporation process and strayed from the LMWL. From June 2013 to June 2014, the EC of the surface water varied from 200 to 600 µS/cm with a chemical facies neutral to HCO_3–Ca (Fig. 13).

Groundwater quality during high water periods

During the high-water-level periods (September 2013, November 2013 and February 2014), some groundwater samples were more depleted ($\delta^{18}O$ and $\delta^{2}H$) than before the monsoon due to mixing with more depleted water (Table 3). During the first stage of the monsoon (i.e. September 2013), the

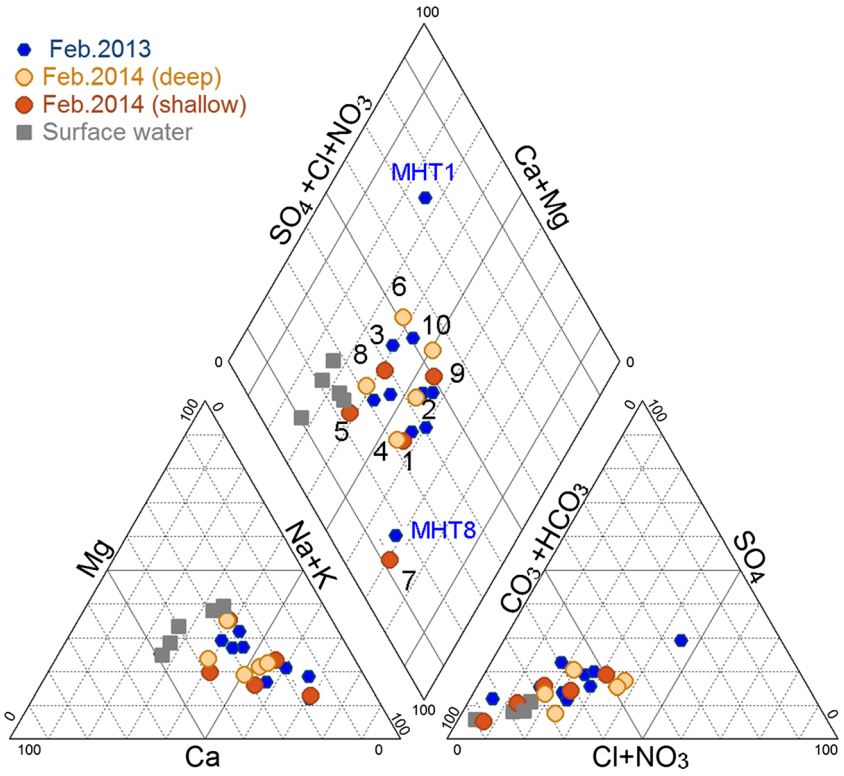

Fig. 13 Piper diagram of the February 2013 and February 2014 groundwater samples and surface water

groundwater samples lined up on the evaporation line of the "dry period" samples (Fig. 12a). The isotopic depletion was not highly noticeable due to the close isotopic facies of the surface water in September 2013. During the second stage of the monsoon (i.e. November 2013 and February 2014), when the surface water was more depleted and the tank extension was more important, some samples deviated from the pre-monsoon values (Fig. 12b, c; Table 3). Mixing lines between the surface water and the groundwater during the "dry period" appeared and the groundwater samples plotted between the two end-points.

For February 2014, the groundwater samples at different depths highlight the strong spatial heterogeneity of the water features (Fig. 11; Table 2; Figs. 12c, 13; Table 3). There was a notable vertical heterogeneity within the boreholes. For MHT3, MHT4 and MHT8 notably, the chemical facies, the EC and the isotope contents are particularly contrasted between the shallow and deep samples.

While the EC values were close for deep samples of some boreholes (MHT2, MHT4, MHT8, MHT9; samples 2, 6, 8 and 10, respectively), their chemical facies and their isotopic signatures were different. Shallow samples of MHT3 and MHT8 (samples 5 and 7) had a very similar EC but showed contrasted isotopic signature and chemical facies (Figs. 11, 12c and 13).

Recharge impact on groundwater quality

There is no general trend in the recharge impact on geochemical parameters. During the high water period, there is no isotopic depletion for every well and there is either a salinization or a dilution of the water (Table 4). The temporal and spatial impact of the recharge on $\delta^{18}O$ is also highly variable.

The comparisons between samples of February 2014 and the pumped samples of 2013 offer good insight into the vertical heterogeneity of the recharge impact (Tables 3 and 4 and Fig. 12c). Some shallow samples underwent a strong influence from mixing with depleted surface water, while deep samples generally line up on the groundwater line highlighted for the "dry condition" on the $\delta^{18}O$ vs $\delta^{2}H$ plot. For example, the shallow samples of MHT3, MHT4 and MHT9 (samples 3, 6 and 9, respectively) are located on mixing lines, while the deep samples are mainly located on the "dry period" line (Fig. 12c). However, compared to the shallow sample of MTH8 (7), the MHT8 deep sample (8) appears to be located on a mixing line between surface water and the shallow sample (7) (Fig. 12c). One notes that the shallow sample of MHT2 (1) is located on the dry condition groundwater line. Consideration of all the information (Figs. 11, 12, 13 and Table 4) allows a full description of the 4 contrasted patterns observed in the MHT:

1. Some wells show a significant decrease of their $\delta^{18}O$ associated with an important decrease of EC: MHT2 during the first stage of the monsoon, MHT3 and MHT4 during the second stage of the monsoon. These boreholes have obviously been influenced by an important mixing with depleted and fresh surface water.
2. An important decrease of the stable isotope contents can also be linked to a slightly higher EC, or a very low decrease of EC. This is the case for MHT4 and MHT8 during the first stage of the monsoon, and for MHT9 during the second stage of the monsoon. In these cases, the direct infiltration must be associated with other processes providing the mineral inputs, which can come from soil leaching that occurred during the percolation or from more mineralized water flushed through a piston flow. These processes were observed both for the early and late stages of the monsoon.
3. During the first stage of the monsoon, isotopic contents of some wells remain stable, while the EC decreases (MHT1, MHT3 and MHT9). This can be explained by the piston-flow process flushing fresh water formerly infiltrated during the monsoon. As the facies of the surface water in the early stage of the wet season was close to the groundwater facies (Fig. 12a), it is possible that no noticeable change occurred in the isotopic content.
4. Finally, some wells remain stable (i.e. MHT5) in the first stage of the monsoon, highlighting that the recharge can have no direct impact on groundwater quality, despite the boreholes being located very close to the percolation tank.

The temporal evolution of the chemical features is of importance for some boreholes. This highlights the variability of the processes, which can depend on water level and/or time. For example, the EC of the shallow part of MHT4 increases from June to September (Figs. 7 and 10) before decreasing in October (Fig. 7), while EC remains stable for the deeper part of the profile. The first increase of EC can be explained by the flush of all soluble minerals during the first stage of the wet season, whereas the decrease of EC in October is due to an additional input of fresh water during the second stage of the monsoon. There can also be a change of the flow paths or the connections between the water bodies with water level as shown by MHT2, for which the EC of the shallow part initially decreases during the first stage of the monsoon (Figs. 7 and 10), then increases during the second stage, while the EC remains stable for the deeper part of the profile.

Discussion

The characterization performed through this study highlights the following points, detailed further in this section: (1) the conductive-fracture density, transmissivity and storage decrease with depth and (2) the physical compartmentalization of the aquifer, dependent on the water level, has a strong impact on the spatial heterogeneity of the water quality, (3)

Table 4 Evolution of the $\delta^{18}O$ (‰ vs SMOW) and relative evolution (%) of the EC between February–September 2013, September–November 2013, and February 2013 and 2014

Borehole	Feb–Sep 2013		Sep–Nov 2013		Feb 2013–Feb 2014				
	$\Delta\ \delta^{18}O$ (‰ vs SMOW)	Relative Δ EC	$\Delta\ \delta^{18}O$ (‰ vs SMOW)	Relative Δ EC (%)	Sample depth	ID	Depth range (m below saprolite)	$\Delta\ \delta^{18}O$ (‰ vs SMOW)	Relative Δ EC
MHT1	−0.1	−25%[a]	NA	NA	MHT1		NA	NA	NA
MHT2	−1.1[a]	−45%[a]	0.5[b]	87%[b]	MHT2: 15 m	1	0–5	−1.7[a]	14%[b]
					MHT2: 40 m[c]	2	25–30	−0.7[a]	20%[b]
MHT3	−0.2	−14%[a]	−7.2[a]	−70%[a]	MHT3: 15 m	3	−5	−4.3[a]	−49%[a]
					MHT3: 30 m[c]	4	10–15	−1.3[a]	−14%[a]
MHT4	−1.5[a]	14%[b]	−2.8[a]	−26%[a]	MHT4: 13 m	5	0–5	−5.5[a]	2 %
					MHT4: 30 m[c]	6	20–25	−1.4[a]	48%[b]
MHT5	−0.2	0 %	NA	NA	MHT5	–	NA	NA	NA
MHT8	−0.7[a]	6 %	NA	NA	MHT8: 18 m	7	−5	−0.5[a]	7 %
					MHT8: 35 m[c]	8	10–15	−1.2[a]	63%[b]
MHT9	−0.1	−11%[a]	−4.1[a]	−9 %	MHT9: 23 m	9	0–5	−3.2[a]	−4 %
					MHT9: 40 m[c]	10	20–25	−2[a]	12%[b]

[a] Decrease of EC or an isotopic depletion

[b] Increase of EC or an isotopic enrichment

[c] Indicates deep samples

the spatial and temporal variability of the recharge impacts the groundwater quality and quantity; and (4) the horizontal flow is a major recharge process at local scale, in contradiction to the usual conceptual model.

Decrease by depth of conductive-fracture density, transmissivity and storage

From this study it is shown that, despite dense fracture networks, few fractures are productive and their density decreases with depth. The reduced sample network (seven boreholes within a site of about 0.3 km^2) remains representative of the crystalline aquifer, as the observations are in accordance with several studies involving numerous observations (e.g. Boutt et al. 2010; Dewandel et al. 2006; Maréchal et al. 2004) where the decrease of conductive fracture density with depth directly impacts the transmissivity and storage of the aquifer; hence the observations on the dynamic evolution discussed hereafter may be applicable elsewhere.

The present work completes the previous studies with the following highlights. It shows that the rare deep fractures may contribute significantly to the general transmissivity of the borehole. It is shown here that this point, usually buffered at the watershed scale, is still valuable at the local scale for the assessment of the impact of MAR structures. As seen for MHT8 and MHT5, some deep conductive fractures play a significant role and can also exhibit quick responses to recharge.

The present work also addresses the temporal component of the groundwater flow paths which has not been studied in detail previously, due to a lack of temporal data. The hydraulic connectivity between the wells increases with the rise of the water level. This is highlighted by the evolution of the number of connected breakpoints in the higher part of the EC profile between the wells. It is shown that the productive zone can be more or less important depending on hydrological conditions, due to the vertical structure of the weathering profile and this evolution has been quantified in this study. As an example, the transmissivity of most of the boreholes (MHT2, MHT4 and MHT5) increases by about 10 times from low to high water periods.

Compartmentalization of the aquifer and spatial heterogeneity of the water quality

It is pointed out that compartmentalization affects the aquifer at a small scale, with chemical contrasts between boreholes less than 100 m apart. The high physical compartmentalization of crystalline aquifers has already been highlighted in similar contexts. For example, at the Gajwel study site, located 100 km away from Maheswaram, hydraulic compartments of 400–500 m were found by Perrin et al. (2011a) for more productive farm wells (hydraulic conductivities of about 10 times higher than for the MHT). The same characteristic distance (350 m) has been found by geostatistical analysis of water levels and pumping tests at Choutuppal, 50 km away from Maheshwaram, during low flow conditions (Guihéneuf et al. 2014). While the observation of physical compartmentalization is not new, this concept is subsequently improved by monitoring the temporal dynamic, by quantifying the number of connected fractures with time in an

original manner. The use of different tools (piezometry, HPFM data, geochemistry, borehole profiles) provides a good balance between accuracy and practicability. The use of geochemical data with different sampling depths and HPFM measurements helped to interpret the EC profiles, which are less costly and much simpler to carry out.

Also, while the vertical connectivity of the horizontal fracture network has been studied previously at other Indian sites in a similar geological context (e.g. Boisson et al. 2015), the behavior of the deepest fractures under confined conditions has not been completely demonstrated, as has been done in Sweden (Rodhe and Bockgard 2006) in a different climatic context and for less weathered profiles. This confined behavior is of importance while developing predictive models. With the present study, through the observation of ambient vertical flow measurements and observation of artesian boreholes, it is shown that this behavior can also occur in the Indian context with well-developed weathered profiles.

The strong chemical stratification of the water column within the boreholes is also highlighted by chemical sampling at different depths and the numerous profiles performed. As a direct consequence of the compartmentalization, the aquifer encompasses distinct and poorly connected water bodies. EC can vary by more than 2,000 μS/cm over 0.3 km^2 and chemical facies are very different for close boreholes. Isotopic contents line up on an evaporation line in a wide range, highlighting the large number of isolated water systems. While chemical heterogeneity has been previously observed at the watershed scale (Negrel et al. 2011; Pettenati et al. 2013; Perrin et al. 2011a), to date, no representative scales and temporal evolution data have been available to determine the relation between the various flow paths, as discussed in the following section.

Spatial and temporal variability of recharge impact on groundwater

Recharge can induce various impacts on groundwater quality, from dilution to mineralization by piston flow or soil leaching. At the scale of the study site, the percolated fresh surface water (EC between 200 and 600 μS/cm) generally does not dilute the water of the observed boreholes. Only the MHT2 and MHT3 boreholes showed a significant decrease of EC coupled with an isotopic depletion. The fact that fresh surface water is not found in most of the boreholes could be explained by (1) the effect of the recharge pattern dominated by piston flow coupled with significant storage in the unsaturated saprolite, as highlighted in several studies (e.g. Ruiz et al. 2010; Van der Hoven et al. 2003), or (2) significant leaching of the unsaturated zone before deep percolation.

Isotopic tracers such as $\delta^{18}O$ and $\delta^{2}H$, are valuable tools to identify the recharge fluxes in heterogeneous systems (Herczeg and Leaney 2011). Groundwater isotopic facies results of complex mixes, hydrological processes and isotopic fractionation occurring at all the stages of the hydrological cycle, especially in the semi-arid context of south-India. The distribution of the surface water is highly discontinuous in time and space. The inherent variability of the isotopic signature of the erratic rainfall (Warrier and Babu 2012) is enhanced by the two contrasted monsoon events occurring in South India (Kumar et al. 2010; Negrel et al. 2011). Finally, the varied evaporation processes occurring in ponds, lakes or paddy enhanced by irrigation return flow processes create strong spatial and temporal variability of the signature of the infiltrated surface water (Negrel et al. 2011; Perrin et al. 2011b; Pettenati et al. 2013). The originality of the present study lies in the use of a well-known input signal of surface water, thanks to the Tumulur tank monitoring, which also allows a spatial identification of the input. The definition of the flow path is therefore possible, which is not the case for most of the previous studies. Coupled isotopic and EC information show that vertical recharge occurs in the superficial part for only a few boreholes. In a few cases, a rapid vertical recharge is associated with the leaching of minerals through the vadose zone. For most of the cases, recharge processes through piston flow lead to mineralization of the borehole water, particularly in the middle of the fractured zone (i.e. between 10 and 20 m under the saprolite). The deepest parts of the boreholes remain mainly inactive.

The multitude of identified processes enhances the spatial and temporal variability of the groundwater signature. The chemistry of each borehole is the result of a unique combination of vertical percolation, piston flow and/or preferential recharge paths. It is then possible to conclude that, despite being very close, each borehole intercepts an isolated part of the aquifer with its own recharge pattern. This study gives a good qualitative oversight of the possible recharge mechanisms. Further investigation on chemistry and isotopes is needed to enable estimates of the intensity of the recharge, the water flow paths and the mixing ratios.

Predominance of piston flow and groundwater horizontal dispersion

Recharge fluxes in semi-arid environments are well known for their strong heterogeneity, especially when associated with fractured aquifers (e.g. de Vries and Simmers 2002; Healy and Cook 2002; Herczeg and Leaney 2011; Scanlon et al. 2006). In Maheshwaram, geochemical investigations highlighted that the aquifer response is a balance between recharge through preferential paths and piston flow. Only a few papers discuss this point (e.g. the study of Sukhija et al. (2003) performed at a different scale).

When aquifers are disconnected, the response to an elevation of the surface-water stage is a balance between the cumulative infiltration over time and the rate at which the water can disperse laterally (Shanafield et al. 2012); thus, the response can be highly variable in space due to the strong heterogeneity

of the media. In this study, the convergence of the breakpoints of EC profiles and the presence of deep horizontal preferential flows point toward the good horizontal hydraulic connectivity within the aquifer. While the anisotropy of the conductive fracture network was highlighted in Maréchal et al. (2004), the detailed spatial definition was unknown. The isotopic contents of the water suggest that the mass transfer from surface water is generally more important for the shallow part of the aquifer, where groundwater has a much more depleted isotopic signature. Rapid local recharge down to depths of 20 m has been shown in a fractured aquifer of Ontario (Canada) by Gleeson et al. (2009). In India, it is usually stated that the upper saprolite buffers the vertical flow except when preserved fractures are present. In this study, it is shown that the rapid reaction of the borehole is associated with horizontal flow; however, deep samples also have a significant isotopic depletion, after a long period of high water levels. Moreover, one borehole (MHT8) shows a more important isotopic depletion in its deeper part and no connection with the surface. These varied observations indicate a good lateral dispersion of the recharge flow and that the groundwater fluxes appear to be highly layered; thus, the horizontal part of the groundwater fluxes plays an important role during the recharge.

Variability of the piezometric responses in fractured aquifers has been studied and some very quick and strong reactions have been noted (e.g. Gleeson et al. 2009 in Ontario; Jiménez-Martínez et al. 2013 in France). However, the distinction between hydraulic response and actual recharge through preferential flow paths has been less investigated, as it requires complementary information, such as isotopic tracer data (Rodhe and Bockgard 2006). In the present study, the hydraulic responses of water levels to rainfall events were quick and showed typical fractured-aquifer heterogeneity. There is a good hydraulic continuum allowing the rapid transfer of pressure after a rain event; however, in many cases, isotopic data demonstrate that there is no significant input from surface water to the groundwater after the recharge period, despite the good reactivity of the borehole. This implies that the mass transfer in the aquifer surrounding these boreholes is very limited and that hydraulic effects are responsible for the rise of water levels. A surface loading effect from saturated thick soils, leading to strong hydraulic responses, has been shown by Rodhe and Bockgard (2006) in Sweden and Gleeson et al. (2009) in Ontario. In the present study, the loading role of the thick soil is played by the saprolite, whereas previous studies show that the hydraulic conductivity in the saprolite is low (e.g. Chilton and Foster 1995; Dewandel et al. 2006; Massuel et al. 2013). Permeameter tests in the saprolite performed by Boisson et al. (2015) present values of 3.4×10^{-8} to 1.2×10^{-7} m s^{-1}. Because of the high porosity, an important storage effect in the saprolite has been observed at several sites, despite the possible existence of preferential flow paths (Ruiz et al. 2010; Van der Hoven et al. 2003).

As previously pointed out by several authors (Gleeson et al. 2009; Herczeg and Leaney 2011; Stiefel et al. 2009), and as the present study confirms, there is a need for coupling water level measurements with geochemical measurements to understand the recharge mechanisms at a local scale in heterogeneous aquifers. Coupled chemical and hydrodynamics information highlights the heterogeneous pattern of the recharge in Maheshwaram watershed. From these observations, the following conceptual models on recharge processes and aquifer functioning can be defined.

Recharge pathways

As shown in the present study, the boreholes intercept different water bodies with contrasted chemistry, and the EC values are generally greater in the deep part of the profile. Figure 14a represents the typical state during dry periods, i.e., long-term water stratification being mainly controlled by the low vertical permeability.

During the recharge period, mixes between surface water and groundwater are variable in space, both vertically and horizontally. It is then possible to identify distinct water bodies within the aquifer which are evolving under various hydrological conditions and recharge-flux structures. In this study, both rapid and slow responses to recharge occur at a very local scale, as found also by Gleeson et al. (2009) in a different climatic context. According to these heterogeneous impacts of the recharge, the typical electrical conductivity (EC) logs show variable patterns such as:

1. Vertical diffuse recharge flux and dilution in the shallower zone of the boreholes due to the high permeability of the upper part of the weathering profile (Fig. 14b). This is observed in boreholes MHT2 and MHT3, located to the west of the tank, and known to be the main beneficiaries of the recharge from the tank (Boisson et al. 2014). This is the usual flow pattern considered at watershed scales (Perrin et al. 2011b) and which has been previously observed for a percolation tank by Massuel et al. (2014).
2. Piston flow associated with preferential fluxes recharge through preserved fractures in the saprolite and the fractured zone, and low diffuse vertical flow through a low permeability soil (Fig. 14c). Water flushed by piston flow can show varied mineralization in time and space, as shown by the contrasts of behavior in MHT2, MHT4 and MHT9 during the first and second stages of the high-water-level period. In some cases, mineralization can be caused by soil leaching or rapid water–rock interaction during the recharge (Fig. 14c).
3. Preferential deep horizontal flow (Fig. 14d) and no diffuse vertical flow. The active zone is deeper than in the general case. This process is clear in the halocline evolution at MHT8. It is confirmed by the isotope contents of the

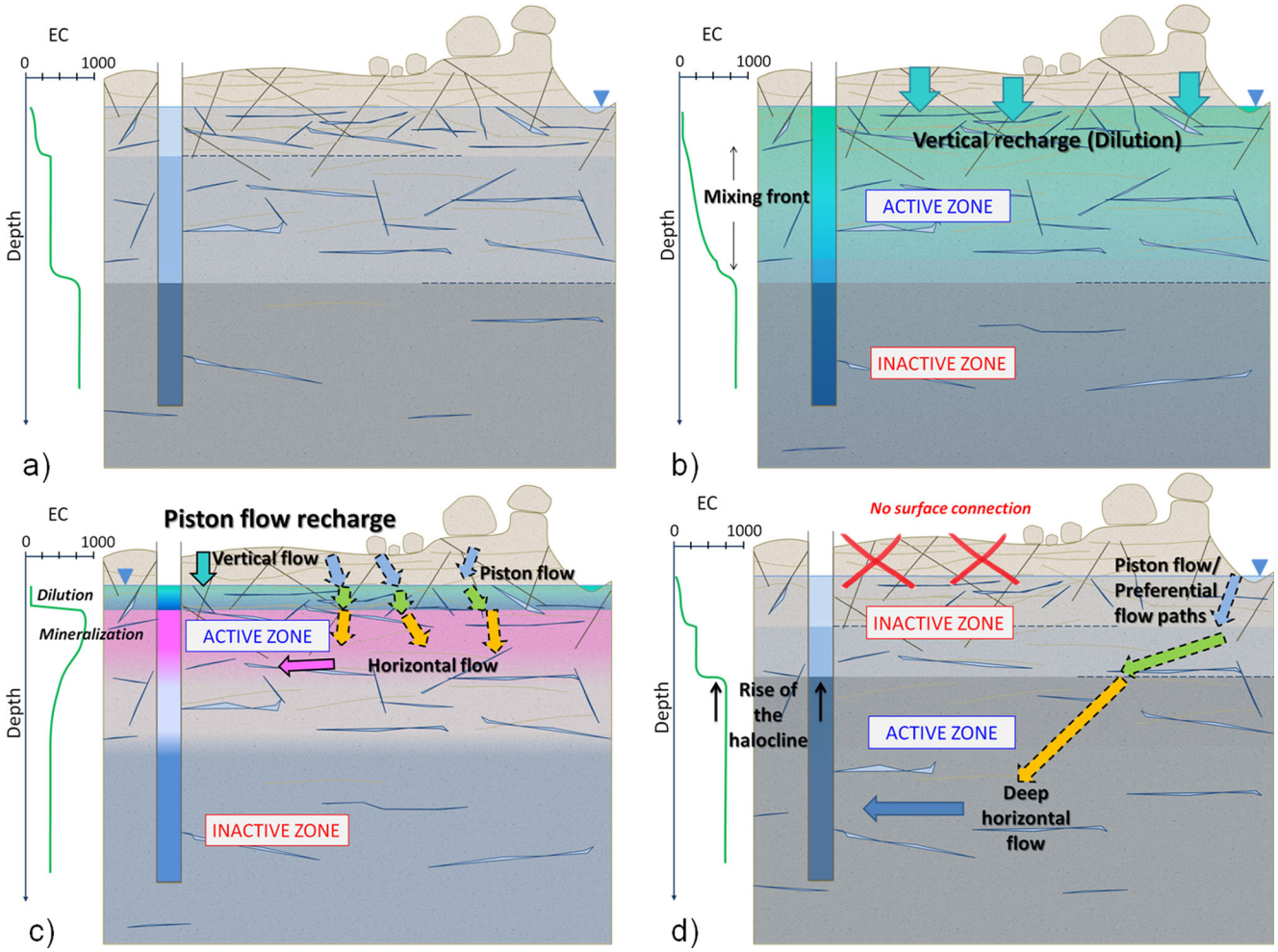

Fig. 14 Different scenarios of recharge, according to soil properties and fractures network, inducing different recharge flow paths. **a** Typical EC profile (μS/cm), intercepting contrasted water bodies during a dry period; **b** vertical diffuse flow; **c** preferential path with a strong horizontal component; **d** deep horizontal flow. The *different colours of the arrows* of piston flow highlight the spatial variability of the chemistry of the flushed water

two layers of water. The deep horizontal flow can also lead to a hydraulic load in the semi confined zone and is then responsible for the artesian condition observed in the MHT2 and MHT3 boreholes during the very high-water-level period.

These contrasted patterns can coexist in an aquifer as well as within a borehole. The present study suggests that recharge can lead to semi-confined behavior of deep fractures and shallow dilution simultaneously (i.e. MHT2 and MHT3 show artesian behavior as well as a shallow dilution). These patterns can also evolve according to the hydrological conditions affecting the connectivity of the flow paths.

Implication for impact assessment of MAR structures

There are MAR projects in crystalline-aquifer contexts across the world, notably in India. One third of India (south) is composed of hard-rock aquifers in an Archean granite context. It is estimated that 0.5 million structures are present in India, with 0.25 million located on crystalline aquifers (Sakthivadivel 2007) and the development will continue (e.g. the Central Ground Water Board of India recommends the construction of 11 million artificial recharge structures). Most of the studies available agree on the lack of local knowledge on the impact of those structures (e.g. Dillon 2009; Glendenning et al. 2012). The key point that must be kept in mind is that these structures, notably in crystalline aquifers contexts, have a local-scale impact only; therefore, large-scale assessment is not appropriate, and the detailed assessment performed in the present study is needed. Comparison with other studies shows that the mechanisms are also applicable elsewhere.

Besides, MAR programs need a lot of funding; hence, the optimization of these structures is of major economical importance. The available project assessments, which incorporate socio economic considerations, are not used in an optimized way due to the lack of technical knowledge on the structure efficiency (Batchelor et al. 2003; Kerr et al. 2002). Firstly,

most of the assessment studies previously performed were based on surface-water balance only. However, the MAR impact on the aquifer is not straight forward, given the low permeability of the saprolite and the anisotropy of the fractured layer. The study described in this report addresses the actual impact of the recharge on the surrounding fractured aquifer in a typical site, for both spatial and temporal aspects.

Conceptual model for aquifer functioning

It is now possible to sum up the general pattern of flow associated with MAR structures and recharge in a fractured aquifer (Fig. 15). This conceptual model brings together the major features of the recharge impacts:

- The presence of partially connected compartments within the aquifer. The existence of contrasted hydraulic heads (dashed lines in Fig. 15) has been highlighted by the natural ambient flow within the boreholes and the water column stratification. The partial hydraulic connection within the different compartments is represented by the colored areas. These connections have been identified by the homogeneous hydraulic responses of the piezometry and the close match between the breakpoints in the EC profiles of the wells.
- A strong compartmentalization of the aquifer with the existence of several water bodies, with distinct EC, chemical facies and isotopic signatures, due to the spatial variability of the surface-water signature, and the different flow paths and mixing rates. These chemical compartments exist because of the low hydraulic conductivity of the media (represented in Fig. 15 with different colors).
- An increase of the stratification of the water column during the recharge period, especially at the top of the fractured layer (boreholes A, B and C in Fig. 15). The water heads of the layers (represented by dashed lines) are shared between more boreholes, and the heads increase during high water levels. This implies an increase of the horizontal connectivity between the boreholes.
- The importance of piston flow and horizontal fluxes resulting in some cases of boreholes with no direct connection with the ground surface (borehole D in Fig. 15). The rise of the water level is ensured by distant connection through deep fractures.

Conclusion

This study addresses the local evolution of flow paths during recharge in fractured crystalline aquifers in relation to

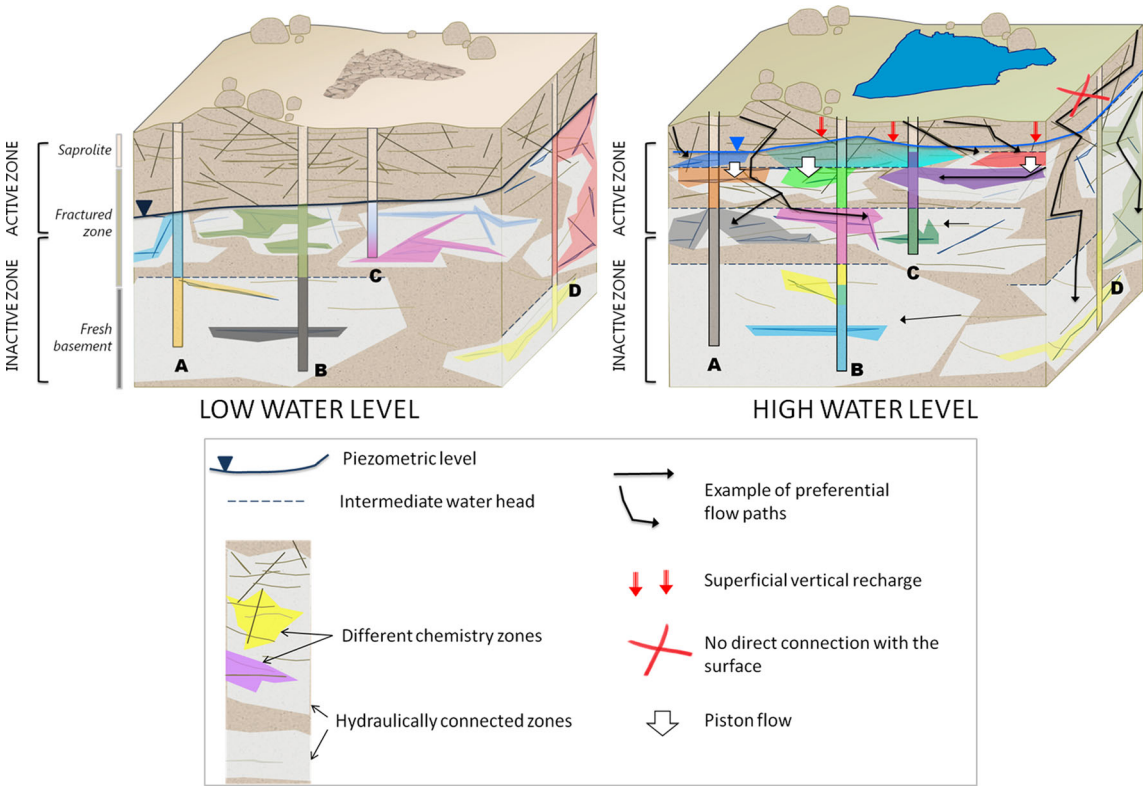

Fig. 15 Conceptual model for aquifer functioning

percolation tanks. The extensive field data (EC logging, water level monitoring, isotopes and major ions) collected throughout the hydrogeological year provides a unique data set allowing the definition of conceptual models on the evolution of recharge processes considering time and depth. The presented results and the conceptual models developed are important in the context of fractured aquifers often used for MAR. They provide valuable information for the assessment and management of MAR structures, water abstraction, the monitoring of the natural recharge in crystalline aquifers, and the assessment of water–rock interaction.

The results highlight (1) the dynamic evolution of the recharge pattern; (2) the layering and stratification with poor vertical mixing; (3) evidence of local compartmentalization with consequences for water chemistry; and (4) the role of the upper active zone as the critical zone for chemical evolution. This latter point is of importance in cases where there is a geogenic contaminant such as fluoride or arsenic. It is moreover crucial that the upper part of the aquifer is the only productive zone in these contexts. This study also evidences the sub-confined behavior of the deepest fractures in short and local scale. The importance of the deep-circulation horizontal flow on water level evolution in boreholes is also highlighted, which was not usually taken into account in most of the previous studies.

The present report gives valuable information at a local scale. Field observations are in good agreement with previous studies on the functioning of these aquifer systems. It is therefore believed that the observed field conditions are representative of crystalline aquifers and that presented concepts can be applicable elsewhere and should be kept in mind while creating or monitoring MAR structures in crystalline aquifers.

Acknowledgements This study was carried out at the Indo-French Center for Ground Water Research (BRGM-NGRI). The authors thank the French Ministry of Foreign Affairs and the Embassy in India for their support. This report has benefited immensely from the detailed comments and improvements provided by the editors and the anonymous reviewers. The authors also wish to acknowledge help from Wajid Uddin and David Villesseche for fieldwork.

References

Acworth RI (1987) The development of crystalline basement aquifers in a tropical environment. Q J Eng Geol Hydrogeol 20:265–272. doi:10.1144/GSL.QJEG.1987.020.04.02

Adhikari RN, Singh AK, Math SKN, Raizada A, Mishra PK, Reddy KK (2013) Augmentation of groundwater recharge and water quality improvement by water harvesting structures in the semi-arid Deccan. Current Sci (Bangalore) 104(11):1534–1542

Athavale RN, Chand R, Rangarajan R (1983) Groundwater recharge estimates for two basins in the Deccan Trap basalt formation / Estimation de la recharge des eaux souterraines de deux bassins dans la formation de basalte du Deccan Trap. Hydrol Sci J 28–4:525–538

Aulong S, Chaudhuri B, Farnier L et al (2012) Are South Indian farmers adaptable to global change? A case in an Andhra Pradesh catchment basin. Reg Environ Chang 12:423–436. doi:10.1007/s10113-011-0258-1

Batchelor CH, Rama Mohan Rao MS, Manohar Rao S (2003) Watershed development: a solution to water shortages in semi-arid India or part of the problem. Land Use Water Resour Res 3:1–10

Boisson A, Baisset M, Alazard M et al (2014) Comparison of surface and groundwater balance approaches in the evaluation of managed aquifer recharge structures: case of a percolation tank in a crystalline aquifer in India. J Hydrol 519(B):1620–1633. doi:10.1016/j.jhydrol.2014.09.022

Boisson A, Guihéneuf N, Perrin J, Bour O, Dewandel B, Dausse A, Viossanges M, Ahmed S, Maréchal JC (2015) Determining the vertical evolution of hydrodynamic parameters in weathered and fractured south Indian crystalline rocks aquifers: insights from a study on an instrumented site. Hydrogeol J. doi:10.1007/s10040-014-1226-x

Bouma JA, Biggs TW, Bouwer LM (2011) The downstream externalities of harvesting rainwater in semi-arid watersheds: an Indian case study. Agric Water Manag 98(7):1162–1170

Boutt DF, Diggins P, Mabee S (2010) A field study (Massachusetts, USA) of the factors controlling the depth of groundwater flow systems in crystalline fractured-rock terrain. Hydrogeol J 18:1839–1854. doi:10.1007/s10040-010-0640-y

Bouwer H, Rice RC (1976) A slug test for determining hydraulic conductivity of unconfined aquifers with completely or partially penetrating wells. Water Resour Res 12(3):423–423

Calder I, Gosain A, Rao MSRM et al (2008) Watershed development in India, 1: biophysical and societal impacts. Environ Dev Sustain 10:537–557. doi:10.1007/s10668-006-9079-7

CGWB (2007) Manual on artificial recharge to groundwater. Central Ground Water Board, New Delhi

CGWB (2009) Dynamic ground water resources of India. Central Ground Water Board, New Delhi

Chilton P, Foster SS (1995) Hydrogeological characterisation and water supply potential of basement aquifers in tropical Africa. Hydrogeol J 3(1):36–49

de Silva CS, Rushton KR (2007) Groundwater recharge estimation using improved soil moisture balance methodology for a tropical climate with distinct dry seasons. Hydrol Sci J 52(5):1051–1067

de Vries JJ, Simmers I (2002) Groundwater recharge: an overview of processes and challenges. Hydrogeol J 10:5–17. doi:10.1007/s10040-001-0171-7

Dewandel B, Lachassagne P, Wyns R et al (2006) A generalized 3-D geological and hydrogeological conceptual model of granite aquifers controlled by single or multiphase weathering. J Hydrol 330:260–284. doi:10.1016/j.jhydrol.2006.03.026

Dillon P (2009) Water recycling via managed aquifer recharge in Australia. Bol Geol Min 120:121–130

Drew L, Shuenemeyer J, Armstrong T, Sutphin D (2001) Initial yield to depth relation for water wells drilled into crystalline bedrocks: Pinardville Quadrangle, New Hampshire. Ground Water 39:676–684

Fishman RM, Siegfried T, Raj P et al (2011) Over-extraction from shallow bedrock versus deep alluvial aquifers: reliability versus sustainability considerations for India's groundwater irrigation. Water Resour Res. doi:10.1029/2011WR010617

Gale IN, Macdonald DMJ, Calow RC, et al (2006) Managed aquifer recharge: an assessment of its role and effectiveness in watershed management. Final report, DFID KAR project R8169, DFID, London

Gleeson T, Novakowski K, Kyser T (2009) Extremely rapid and localized recharge to a fractured rock aquifer. J Hydrol 376:496–509

Glendenning CJ, Van Ogtrop FF, Mishra AK, Vervoort RW (2012) Balancing watershed and local scale impacts of rain water harvesting in India: a review. Agric Water Manag 107:1–13. doi:10.1016/j.agwat.2012.01.011

Gore KP, Pendke MS, Gurunadha Rao VVS, Gupta CP (1998) Groundwater modelling to quantify the effect of water harvesting structures in Wagarwadi watershed, Parbhani district, Maharashtra, India. Hydrol Process 12:1043–1052. doi:10.1002/(SICI)1099-1085(19980615)12:7<1043::AID-HYP638>3.0.CO;2-I

Guihéneuf N, Boisson A, Bour O et al (2014) Groundwater flows in weathered crystalline rocks: impact of piezometric variations and depth-dependent fracture connectivity. J Hydrol 511:320–334. doi:10.1016/j.jhydrol.2014.01.061

Healy RW, Cook PG (2002) Using groundwater levels to estimate recharge. Hydrogeol J 10:91–109. doi:10.1007/s10040-001-0178-0

Herczeg AL, Leaney FW (2011) Review: environmental tracers in arid-zone hydrology. Hydrogeol J 19:17–29. doi:10.1007/s10040-010-0652-7

Jiménez-Martínez J, Longuevergne L, Le Borgne T et al (2013) Temporal and spatial scaling of hydraulic response to recharge in fractured aquifers: insights from a frequency domain analysis: temporal and spatial scaling in fractured aquifers. Water Resour Res 49:3007–3023. doi:10.1002/wrcr.20260

Kerr J, Pangare G, Pangare VL (2002) Watershed development project in India: an evaluation. International Food Policy Research Institute, Washington, DC

Kumar MD, Gosh S, Patel A, Singh OP, Ravindranath R (2006) Rainwater harvesting in India: some critical issues for basin planning and research. Land Use Water Resour Res 6:1–17

Kumar MD, Patel A, Ravindranath R, Singh OP (2008) Chasing a mirage: water harvesting and artificial recharge in naturally water-scarce regions. Econ Polit Wkly 43:61–71

Kumar SB, Rai P, Saravana Kumar U et al (2010) Isotopic characteristics of Indian precipitation. Water Resour Res 46:W12548. doi:10.1029/2009WR008532

Maréchal JC, Dewandel B, Subrahmanyam K (2004) Use of hydraulic tests at different scales to characterize fracture network properties in the weathered-fractured layer of a hard rock aquifer: fracture network properties in hard rock. Water Resour Res 40. doi: 10.1029/2004WR003137

Maréchal JC, Dewandel B, Ahmed S et al (2006) Combined estimation of specific yield and natural recharge in a semi-arid groundwater basin with irrigated agriculture. J Hydrol 329:281–293. doi:10.1016/j.jhydrol.2006.02.022

Massuel S, George BA, Venot J-P, Bharati L, Acharya S (2013) Improving assessment of groundwater-resource sustainability with deterministic modelling: a case study of the semi-arid Musi subbasin, South India. Hydrogeol J. doi:10.1007/s10040-013-1030-z

Massuel S, Perrin J, Mascre C et al (2014) Managed aquifer recharge in South India: what to expect from small percolation tanks in hard rock? J Hydrol 512:157–167. doi:10.1016/j.jhydrol.2014.02.062

Metha M, Jain S K (1997) Efficiency of artificial recharge from percolation tanks. In Simmers I (ed) Recharge of phreatic aquifers in (semi-)arid areas. IAH Int. Contrib. Hydrogeol. 19, Taylor and Francis, London, pp 271–277

Mukherji A, Shah T (2005) Groundwater socio-ecology and governance: a review of institutions and policies in selected countries. Hydrogeol J 13:328–345. doi:10.1007/s10040-005-0434-9

Negrel P, Pauwels H, Dewandel B et al (2011) Understanding groundwater systems and their functioning through the study of stable water isotopes in a hard-rock aquifer (Maheshwaram watershed, India). J Hydrol 397:55–70

Oblinger JA, Moysey SMJ, Ravindrinath R, Guha C (2010) A pragmatic method for estimating seepage losses for small reservoirs with application in rural India. J Hydrol 385:230–237. doi:10.1016/j.jhydrol.2010.02.023

Paillet FL (1998) Flow modeling and permeability estimation using borehole flow logs in heterogeneous fractured formations. Water Resour Res 34:997–1010

Perrin J, Ahmed S, Hunkeler D (2011a) The effects of geological heterogeneities and piezometric fluctuations on groundwater flow and chemistry in a hard-rock aquifer, southern India. Hydrogeol J 19:1189–1201. doi:10.1007/s10040-011-0745-y

Perrin J, Mascré C, Pauwels H, Ahmed S (2011b) Solute recycling: an emerging threat to groundwater quality in southern India? J Hydrol 398:144–154

Pettenati M, Perrin J, Pauwels H et al (2013) Simulating fluoride evolution in groundwater using a reactive multicomponent transient transport model: application to a crystalline aquifer of southern India. Appl Geochem 29:102–116

Pettenati M, Picot-Colbeaux G, Thiéry D et al (2014) Water quality evolution during Managed Aquifer Recharge (MAR) in Indian crystalline basement aquifers: reactive transport modeling in the critical zone. Proc Earth Planet Sci 10:82–87. doi:10.1016/j.proeps.2014.08.016

Rangarajan R, Athavale RN (2000) Annual replenishable ground water potential of India: an estimate based on injected tritium studies. J Hydrol 234:38–53

Rodhe A, Bockgard N (2006) Groundwater recharge in a hard rock aquifer: a conceptual model including surface-loading effects. J Hydrol 330:389–401

Ruiz L, Varmac MRR, Kumar MSM, Sekhar M, Maréchal JC, Descloitres M, Riotte J, Kumar S, Kumar C, Braun JJ (2010) Water balance modelling in a tropical watershed under deciduous forest (Mule Hole, India): regolith matric storage buffers the groundwater recharge process. J Hydrol 380:460–472

Saha D, Dwivedi SN, Roy GK, Reddy DV (2013) Isotope-based investigation on the groundwater flow and recharge mechanism in a hard-rock aquifer system: the case of Ranchi urban area, India. Hydrogeol J 21:1101–1115

Sakthivadivel R (2007) The groundwater recharge movement in India. In: Giordano M, Villholth KG (eds) The agricultural groundwater revolution: opportunities and threats to development. CABI, Wallingford, UK

Scanlon BR, Tyler SW, Wierenga PJ (1997) Hydrologic issues in arid, unsaturated systems and implications for contaminant transport. Rev Geophys 35(4):461–490

Scanlon BR, Keese KE, Flint AL, Flint LE, Gaye CB, Edmunds WM, Simmers I (2006) Global synthesis of groundwater recharge in semi-arid and arid regions. Hydrol Process 20:3335–3370

Shah T (2009) Taming the anarchy: groundwater governance in South Asia. Earthscan, London, 310 pp

Shanafield M, Cook PG, Brunner P et al (2012) Aquifer response to surface water transience in disconnected Streams. Water Resour Res 48:W11510. doi:10.1029/2012WR012103

Simmers I (1997) Groundwater recharge principles, problems and developments. In: Simmers I, Hendrickx JMH, Kruseman GP, Rushton KR (eds) Recharge of phreatic aquifers in (semi-) arid areas. IAH, Wallingford, UK; Balkema, Rotterdam, The Netherlands

Stiefel JM, Melesse AM, McClain ME et al (2009) Effects of rainwater-harvesting-induced artificial recharge on the groundwater of wells in Rajasthan, India. Hydrogeol J 17:2061–2073. doi:10.1007/s10040-009-0491-6

Sukhija BS, Reddy DV, Nagabhushanam P, Hussain S (2003) Recharge processes: piston flow vs preferential flow in semi-arid aquifers of India. Hydrogeol J 11:387–395. doi:10.1007/s10040-002-0243-3

Sukhija BS, Reddy DV, Nagabhushanam P et al (2006) Characterisation of recharge processes and groundwater flow mechanisms in

weathered-fractured granites of Hyderabad (India) using isotopes. Hydrogeol J 14:663–674

Van der Hoven SJ, Solomon DK, Moline GR (2003) Modeling unsaturated flow and transport in the saprolite of fractured sedimentary rocks: effects of periodic wetting and drying: modeling unsaturated flow and transport. Water Resour Res 39. doi: 10.1029/2002WR001926

Warrier CU, Babu MP (2012) A study on the spatial variations in stable isotopic composition of precipitation in a semiarid region of southern India. Hydrol Process 26:3791–3799. doi:10.1002/hyp.8453

White AF, Bullen TD, Schulz MS, Blum AE, Huntington TG, Peters NE (2001) Differential rates of feldspar weathering in granitic regoliths. Geochem Cosmochem Acta 65-6: 847–869

Wyns R, Baltassat JM, Lachassagne P et al (2004) Application of SNMR soundings for groundwater reserves mapping in weathered basement rocks (Brittany, France). Bull Soc Geol Fr 175(1): 21–34